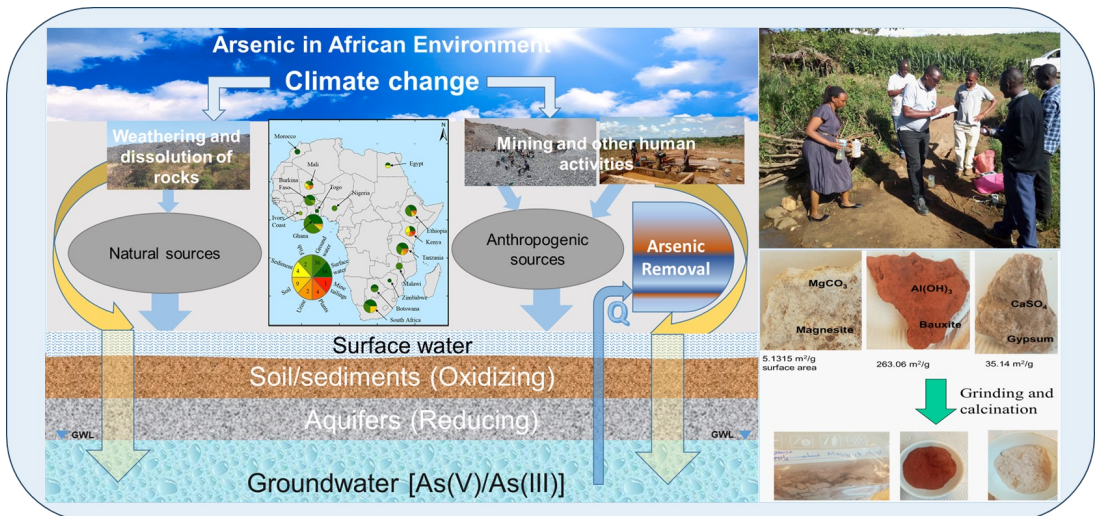


Doctoral Thesis in Land and Water Resources Engineering

Treatment of arsenic contaminated drinking water from the sources around the gold mining areas of Geita and Mara, Tanzania

Removal efficiency of locally available materials, bauxite, gypsum, and magnesite

REGINA FILEMON IRUNDE



Treatment of arsenic contaminated drinking water from the sources around the gold mining areas of Geita and Mara, Tanzania

Removal efficiency of locally available materials, bauxite, gypsum, and magnesite

REGINA FILEMON IRUNDE

Academic Dissertation which, with due permission of the KTH Royal Institute of Technology, is submitted for public defence for the Degree of Doctor of Technology on Tuesday the 19th December 2023, at 1:00 PM at Room Sahara, Teknikringen 10B, KTH, Stockholm.

Doctoral Thesis in Land and Water Resources Engineering
KTH Royal Institute of Technology
Stockholm, Sweden 2023

© Regina Filemon Irunde

Cover page photo and illustration: The overview of arsenic in the African continent, the natural and anthropogenic sources and occurrences in groundwater environment. The right panel shows the natural minerals bauxite, gypsum and magnesite which are used for removal of arsenic from water sources as well as a photograph of the campaign for groundwater sampling in the field.

ISBN 978-91-8040-779-3
TRITA-ABE-DLT-2351

Printed by: Universitetservice US-AB, Sweden 2023

dafwat



Sweden

Sverige



© 2023 Regina Filemon Irunde

PhD Thesis

KTH International Groundwater Arsenic Research Group

Water and Environmental Engineering

Department of Sustainable Development, Environmental Science and Engineering

School of Architecture and Built Environment

KTH Royal Institute of Technology

SE-100 44 STOCKHOLM, Sweden

Reference should be written as:

Irunde, R.F. (2023) Treatment of arsenic contaminated drinking water sources around the gold mining areas of Geita and Mara, Tanzania: Removal efficiency of locally available materials, bauxite, gypsum, and magnesite. PhD Thesis, TRITA-ABE-DLT-2351, 54p.

DEDICATION

*To
My Parents, Siblings
and
Nephews*

The pH of the water is an important parameter for As mobilization in the environment; it changes the surface charge of an adsorbent (Chen et al., 2016)

SAMMANFATTNING

Under de senaste åren har höga halter av arsenik (As) på cirka 300 µg/L rapporterats runt guldgruveområdena i Geita- och Mara-regionerna i Victoriasjöns avrinningsområde (LVB) i Tanzania. Under provtagningskampanjen vid Geita och Mara visade grundvatten- och ytvattenproverna förekomst av höga As-koncentrationer samt Fe och sulfid. Flera brunnar överges på grund av lukt orsakad av högt innehåll av sulfid, liksom röd färg, på grund av hög järnhalt. Cirka 53 % av de analyserade vattenproverna överskred WHO:s riktlinjer för dricksvatten. Frisättningen av As tillskrivs främst vittring av sulfidmineraler som arsenopyrit i samband med guldbrytningen. I vissa delar av LVB rapporteras allt fler cancerfall och kliniska undersökningar står nu på den nationella agendan för att identifiera möjliga orsaker.

Vattenrening med bauxit, gips och magnesit visar lovande resultat, särskilt bauxit och magnesit kan sänka As-koncentrationerna till under 0.1 µg/L. Både bauxit och magnesit fungerade effektivt för As-avlägsnande även vid högre koncentrationer över 5 mg/L, medan gips är att föredra för behandling av låga As-koncentrationer. Dessutom hade magnesit en unik kemisk karaktär för att påverka andra material att ha hög effektivitet vid As-borttagning; Det höjer dock vattnets pH upp till 10. Vid tillsats av 5 g/L magnesit i vatten med 5 mg/L As, kan As halten sänkas till under 10 µg/L inom 30 min. As-borttagningen ökade med dosering och kontakttid upp till 98 % efter 4 timmar, vilket är i överensstämmelse med Visual MINTEQ-simulering. Prestandan hos kalcinerad magnesit och gips passade väl med Freundlich-adsorptionsisoterm, som indikerar närvaron av kemisk reaktion som styrande faktor för As-avlägsnande medan bauxit stämde med Langmuir-isoterm, vilket indikerar yttäckning i ett lager. De kinetiska reaktionerna observerades följa pseudo andra ordningen. Statistiken följer linjär regression med R^2 som sträcker sig mellan 0.7 och 0.9. Det artificiella neurala nätverket avslöjade pH som en av de mest inflytelserika parametrarna för avlägsnande av As från vatten. En kolumn i liten skala med en flödeshastighet på 0.5 – 1 mL/min under 30 minuter visade en adsorptionskapacitet mellan 0.07 och 0.14 µg/g som följer Thomas linjära modell med hastighetskonstanten k_{TH} på 29.48 till 211.25 mL/min µg.

Frisättning av element från förbrukad magnesit, gips och bauxit såsom magnesium (Mg), aluminium (Al), järn (Fe), kalcium (Ca) visade sig ligga under WHO:s standarder efter vattenrening. Desorptionsprocessen av As från förbrukad magnesit och gips var dock en utmaning, vilket innebär att det bildades en stark bindning mellan Mg-O-As och Ca-O-As.

Denna studie är baserad på 5 artiklar som ger betydande insikter till forskare, beslutsfattare och samhället runt As-förorenade platser för att lära sig om förekomsten av As och enkla saneringstekniker som utvärderas i denna studie.

Nyckelord: Arsenik; bauxit; gips; magnesit; naturligt vatten; rening; Visual MINTEQ; kinetisk reaktion; isotermer; Freundlich; Langmuir.

IKISIRI

Katika miaka ya hivi karibuni, viwango vya juu vya As vya 300 $\mu\text{g}/\text{L}$ vinaripotiwa karibu na maeneo ya uchimbaji wa dhahabu ya mkoa ya Geita na Mara ndani ya bonde la Ziwa Victoria (LVB) nchini Tanzania. Wakati wa kampeni ya sampuli katika mkoa ya Geita na Mara, sampuli za maji ya ardhini na maji ya mito zilifichua uwepo wa viwango vya juu vya As pamoja na Fe na sulfide. Visima kadhaa vimeachwa kwa sababu ya harufu kutokana na sulfide iliyomo kwenye maji, pamoja na rangi nyekundu, kwa sababu ya chuma. Karibu 53% ya sampuli za maji zilizochambuliwa zilizidi mwongozo wa WHO wa maji ya kunywa. Kutolewa kwa As kimsingi kunahusishwa na hali ya hewa ya madini ya sulfide kama arsenopyrite inayohusiana na shughuli za madini ya dhahabu. Katika baadhi ya maeneo ya LVB, idadi kubwa ya kesi za saratani zinaripotiwa na uchunguzi wa kliniki sasa uko kwenye ajenda ya kitaifa ya kutambua sababu zinazowezekana.

Matibabu ya maji kwa kutumia bauxite, gypsum na magnesite inaonyesha matokeo ya kuahidi, hasa bauxite na magnesite inaweza kupunguza viwango vya As mpaka chini ya 0.1 $\mu\text{g}/\text{L}$. Wote bauxite na magnesite walifanya kazi kwa ufanisi juu ya As kuondolewa hata katika viwango vya juu ya 5 mg/L wakati gypsum ni bora kwa matibabu ya viwango vya chini vya As kwenye maji. Zaidi ya hayo, magnesite alikuwa na tabia ya kipekee ya kemikali kushawishi nyenzo zingine kuwa na ufanisi mkubwa juu ya As kuondolewa; hata hivyo huinua pH ya maji hadi 10. Baada ya kuongeza 5 g/L magnesite katika 5 mg/L As, inaweza kupunguza As chini ya 10 $\mu\text{g}/\text{L}$ ndani ya dakika 30. Kuondolewa kwa As iliongezeka hadi 98% kulingana na kipimo cha madini kuongezeka, pia na wakati wa maji kugusana katika masaa 4 ambayo inakubaliana na simulation ya Visual MINTEQ. Utendaji wa magnesite iliyochoywa, na gypsum ulioneshwa vizuri na Freundlich adsorption isotherm, ambayo inaonyesha uwepo wa majibu ya kemikali kama sababu ya kudhibiti kwa As kuondolewa wakati bauxite ilifaa vizuri kwenye Langmuir isotherm inayoonyesha chanjo ya uso wa monolayer. Mwitikio wa kinetic ulizingatiwa kufuata utaratibu wa pili wa pseudo. Takwimu hutii regression ya mstari na R^2 kuanzia kati ya 0.7 na 0.9. Mtandao wa neva bandia ulifunua pH kama kigezo cha kushawishi zaidi kwa As kuondolewa kutoka kwa maji. Safu ndogo ilifunua kiwango cha mtiririko wa 0.5 - 1 mL/min kwa dakika 30 na uwezo wa mtiririko kati ya 0.07 na 0.14 $\mu\text{g}/\text{g}$ ambayo inatii mfano wa Thomas linear na kiwango cha mara kwa mara cha k_{TH} ya 29.48 hadi 211.25 $\text{mL}/\text{min } \mu\text{g}$.

Kutolewa kwa vitu kutoka kwa magnesite iliyotumika, gypsum, na bauxite kama vile magnesiamu (Mg), alumini (Al), chuma (Fe), kalsiamu (Ca) ilipatikana kuwa chini ya viwango vya WHO baada ya matibabu ya maji. Hata hivyo, mchakato wa kuiachanisha As kutoka kwa magnesite iliyotumika na gypsum ilikuwa changamoto ambayo inamaanisha kulikuwa na muungano mgumu kati ya Mg-O-As na Ca-O-As.

Utafiti huu unategemea machapisho 5 ambapo utachangia ufahamu muhimu kwa jamii ya kisayansi, watunga sera na jamii inayoishi karibu na maeneo yaliyochafuliwa, kujifunza kuhusu matukio ya uchafuzi wa vyanzo vya maji pamoja na mbinu rahisi za kuondoa As zilizotathminiwa katika utafiti huu.

Istilahi muhimu: Arseniki; bauxite; gypsum; magnesite; maji ya asili; kuondolewa; Visual MINTEQ; misugano ya kinetic; isotherm; Freundlich; Langmuir.

ACKNOWLEDGMENTS

Special thanks to my supervisors, **Professor Prosun Bhattacharya** of KTH Royal Institute of Technology and **Professor Felix Mtalo** of the University of Dar es Salaam, for their tireless supervision and guidance during my doctoral study. I remember when Professor Mtalo insisted me to attend an interview to join the Sida program, and that was the first time I met Professor Prosun Bhattacharya at the interview. It was an intensive interview where all candidates presented their proposals on water quality, arsenic, and fluoride removal, through which, I was selected to join the DAFWAT project. **Prof. Joydeep Dutta** and the team at FNM-Lab KTH, thank you for your lab facility support during 2019 and 2020.

The Swedish International Development cooperation Agency (**Sida**), thank you for funding this study under DAFWAT project 2235, which is a collaboration between KTH-Sweden and the University of Dar es Salaam, Tanzania. ISP Uppsala, the November 2022 committee under **Peter Sundin** thank you for your time and support during my study in Sweden. **Archana Ganganaboina** and **Dr. Latifa Mbelwa** thank you for your support on allowance issues during my stay in Sweden.

KTH. The head of SEED, **Maria Malmström**, thank you for your support and review of my work in 2022. All **SEED staff** and **students**, thank you for your warm greetings in the corridors. **Dr. Agnieszka** and **Prof. Gunno Renman** thank you for the support in the laboratory, you were always there on time when I needed help. **Dr. Elias Azzi**, thank you for your encouragement. **Sigvad Bast**, thank you for all the times at fika. **Arman**, thank you for the support of transparent pipes for my mini-scale column experiment.

Dr. Rajabu Hamisi, you bought lunch for me and Fina on the first day in Sweden when we didn't have any kronor in our pocket, thank you also for your technical support during my study. **Suzanne**, thank you for the accommodation in 2017 and 2019, also the delicious African food. **Blandina and Martin**, thank you for the accommodation in 2021 and delicious cakes. **Rehema and Angela Ribberheim**, thank you for everything and accommodation in summer 2022 and 2023, I have enjoyed learning farm skills and eating fresh green vegetables from your farm.

The family of **Prof. Linley** and **Erik Karlton**, thank you for your support, free accommodation, counselling, and great moments we shared during my stay in your house during March - June 2023. I will miss the delicious food made by Prof Erik and the spicy food with much pilipili made by Prof. Linley. Prof. Erik Karlton, thank you again for your coaching on how to report results scientifically which made my way to a scientific publication.

My **parents, brothers, sisters, and nephews** in Tanzania, thank you for your encouragement and prayers. **Mama Elizabeth** in UK, thank you for your prayers and counselling. DAFWAT fellows **Dr. Vivian, Dr. Julian, Dr. Fanuel**, thank you for the time we shared at KTH. **Dr. Mtamba** thank you. **Mr. Ulomi**, thank you for your support at WRE Lab. **All Sida students**, thank you. **Dr. Rakesh Kumar** of Auburn University, USA, thank you for the preliminary thesis review. Special thanks to **Prof. Rachel Pettersson** of KTH for critical review of the thesis.

Regina Irunde
Stockholm, December 2023

LIST OF SYMBOLS AND ABBREVIATIONS

Adj. R^2	Adjusted correlation coefficient
As	Arsenic
ASM	Artisanal and small-scale gold mining
BGM	Bauxite, gypsum, and magnesite in layers
F	Distribution of data in statistics
g/L	gram per liter
h	Hours
ICP-OES	Inductively coupled plasma optical emission spectroscopy
kV	kilovolt
LVB	Lake Victoria Basin
mA	milliamper
mg/L	milligram per liter
$\mu\text{g/L}$	microgram per liter
min	minutes
mL	milliliter
<i>p</i> -value	probability value
rpm	Revolutions per minute
=SH	Sulfhydryl group
std	Standard error
t	time
r	Correlation coefficient
R^2	Correlation coefficient of fit
URT	United Republic of Tanzania

LIST OF APPENDED PAPERS

This dissertation was developed based on the following five papers:

- I. **Irunde, R.**, Ijumulana, J., Ligate, F., Maity, J.P., Ahmad, A., Mtamba, J., Mtalo, F., Bhattacharya, P. 2022. Arsenic in Africa: Potential sources, spatial variability, and the state of the art for arsenic removal using locally available materials. *Groundwater for Sustainable Development* 18:100746. <https://doi.org/10.1016/j.gsd.2022.100746>
- II. Ligate, F., Lucca, E., Ijumulana, J. **Irunde, R.**, Kimambo, V., Bhattacharya, P., Mtalo, F., Ahmad, A., Hamisi, R., and Maity, J., 2022. Geogenic contaminants and groundwater quality around Lake Victoria goldfields of Northwestern Tanzania. *Chemosphere* 307: 135732. <https://doi.org/10.1016/j.chemosphere.2022.135732>
- III. **Irunde, R.**, Ligate, F.J., Ijumulana, J., Ahmad, A., Maity, J.P., Hamis, R., Philip, J.Y.N., Kilulya, K.F., Karlun, E., Mtamba, J., Bhattacharya, P., Mtalo, F., 2023. The natural magnesite efficacy on arsenic extraction from water and alkaline influence on metal release in water. *Applied Geochemistry* 155: 105705.: <https://doi.org/10.1016/j.apgeochem.2023.105705>
- IV. **Irunde, R.**, Ligate, F.J., Ijumulana, J., Kumar, R., Maity, J., Bhattacharya, P., Mtalo, F., 2023. Bauxite: A prospective mineral for arsenic elicitation from water and acidic influence. *Surfaces and Interfaces* (Manuscript under review).
- V. **Irunde, R.**, Ligate, F.J., Ijumulana, J., Bhattacharya, P., Mtalo, F., 2023. Gypsum application for arsenic uptake from water. *Journal of Hazardous Materials Advances* (Manuscript under review).

Author's contribution to papers

I contributed to the papers included and appended in the thesis as follows:

- I. Created the concept of the manuscript, collected data, wrote the manuscript, and corrected the manuscript from co-authors inputs, and Julian Ijumulana helped with data modelling using GIS to obtain the results represented in section 2. Initiated submission to the journal and all publication processes.
- II. Contributed to the field work, data collection, result interpretation, chemical speciation using Visual MINTEQ, writing, and manuscript revision. The first author enhanced the writing and was responsible for submission to the journal and publication process.
- III. Conceptualization of the manuscript, field work, setting experiments, sample analysis, interpretation of the data, writing the manuscript, revising the manuscript from co-authors inputs, and progressing with publication.
- IV. Conceptualization of the manuscript, field work, setting experiments, sample analysis, interpretation of the data, writing the manuscript, revising the manuscript from co-authors inputs, and journal submission process.
- V. Conceptualization of the manuscript, field work, setting experiments, sample analysis, interpretation of the data, writing the manuscript, revising the manuscript from co-authors inputs, and journal submission process.

The original papers are reproduced in this thesis with permission from the respective publishers.

LIST OF OTHER RELEVANT PAPERS NOT APPENDED TO THIS THESIS

- I. Ijumulana, J., Ligate, F., **Irunde, R.**, Bhattacharya, P., Maity, J.P., Ahmad, A. & Mtaló, F. 2021. Spatial uncertainties in fluoride levels and health risks in endemic fluorotic regions of northern Tanzania. *Groundwater for Sustainable Development* 14: 100618. <https://doi.org/10.1016/j.gsd.2021.100618>
- II. Ligate, F.J., Ijumulana, J., Ahmad, A., Kimambo, V., **Irunde, R.**, Mtamba, J.O., Mtaló, F. & Bhattacharya, P. 2021. Groundwater resources in the East African Rift Valley: Understanding the geogenic contamination and water quality challenges in Tanzania. *Scientific African* 13: e00831. <https://doi.org/10.1016/j.sciaf.2021.e00831>
- III. Ijumulana, J., Ligate, F., **Irunde, R.**, Bhattacharya, P., Ahmad, A., Tomašek, I., Maity, J.P., Mtaló, F. 2022. Spatial variability of the sources and distribution of fluoride in groundwater of the Sanya alluvial plain aquifers in northern Tanzania. *Science of The Total Environment* 810: 152153. <https://doi.org/10.1016/j.scitotenv.2021.152153>
- IV. Ligate, F.J., Ijumulana, J., **Irunde, R.**, Kimambo, V., Hamisi R., Maity J.P., Mtamba J.O., Mtaló F. & Bhattacharya, P. 2023. Hydrogeochemistry and spatial variability of arsenic and fluoride co-occurrence in groundwater from Geita district in Lake Victoria Basin, northwest Tanzania. *Groundwater for Sustainable Development* (GSD-23-00042, Manuscript in revision)

TABLE OF CONTENTS

<i>Sammanfattning</i>	<i>ix</i>
<i>IKISIRI</i>	<i>xi</i>
<i>Acknowledgments</i>	<i>xiii</i>
<i>List of Symbols and abbreviations</i>	<i>xv</i>
<i>List of Appended Papers</i>	<i>xvii</i>
<i>List of other relevant papers not appended to this thesis</i>	<i>xviii</i>
<i>Table of contents</i>	<i>xix</i>
Abstract	1
1. Introduction	2
2. Aims, objectives, and research questions	2
2.1. Rationale	2
2.2. Objectives and research questions	3
2.2.1. General objective.....	3
2.2.2. Specific objectives	3
2.2.3. Research questions.....	3
2.3. Scope of the study	3
2.4. Thesis structure	3
3. Background	3
3.1. Mining activities in Geita and Mara	4
3.2. Arsenic	4
3.2.1. Field measurements of Arsenic.....	4
3.2.2. Laboratory measurements.....	5
3.2.3. Arsenic removal techniques	6
3.3. Factors affecting arsenic adsorption efficiency	6
3.3.1. Initial As concentration.....	6
3.3.2. Adsorbent dosage.....	6
3.3.3. pH.....	6
3.3.4. Contact time.....	6
4. Methods	6
4.1. Study area	6
4.2. Collection of water samples and the local adsorbents	7
4.2.1. Collection of water samples	7
4.2.2. Collection of local adsorbents bauxite, gypsum, and magnesite.....	8
4.2.3. Sample treatment and analysis.....	8
4.2.4. Preparation of adsorbent materials.....	8
4.3. Water treatment for arsenic removal	9
4.3.1. Bauxite (Paper IV).....	9
4.3.2. Gypsum (Paper V).....	10
4.3.3. Magnesite (Paper III).....	10
4.4. Mini-scale column experiment	11
4.5. Theoretical calculations	11
5. Results	14
5.1. Arsenic occurrence and contamination in the environment (Papers I & II).	14
5.1.1. Occurrence (Paper I)	14
5.2. Evaluation of water sample characteristics in Geita and Mara (Paper II)	15

5.3.	Removal technologies using bauxite, gypsum, and magnesite (<i>Papers III, IV & V</i>).....	16
5.3.1.	Magnesite (Paper III).....	17
5.3.2.	Bauxite (Paper IV).....	24
5.3.3.	Gypsum. (Paper V).....	33
5.4.	The mini-scale column experiment	41
5.5.	Natural factors that control arsenic in lake Victoria basin.....	44
6.	<i>Discussion</i>	44
6.1.	Occurrence of arsenic (<i>Paper I</i>).....	44
6.2.	Geochemical evaluation of water (<i>Paper II</i>).....	44
6.3.	Magnesite (<i>Paper III</i>).....	45
6.4.	Bauxite (<i>Paper IV</i>).....	46
6.5.	Gypsum (<i>Paper V</i>).....	47
6.6.	Mini-scale column evaluation.....	48
6.7.	Natural mitigation of Aresnic.....	48
7.	<i>Conclusions</i>	49
8.	<i>References</i>	49

ABSTRACT

In recent years, high arsenic (As) levels of about 300 $\mu\text{g/L}$ have been reported around the gold mining areas of Geita and Mara regions within the Lake Victoria basin (LVB) in Tanzania. During a sampling campaign at Geita and Mara, the groundwater and surface water samples revealed the presence of high As concentrations as well as Fe and sulfide. Several wells are abandoned because of odor due to high content of sulfide, as well as red color, due to high iron content. About 53% of the analyzed As water samples exceeded the WHO guideline for drinking water. The release of As is primarily attributed to the weathering of sulfide minerals like arsenopyrite related to gold mining activities. In some parts of the LVB, an increasing number of cancer cases are being reported, and clinical investigations are now on the national agenda to identify the possible causes.

Water treatment using bauxite, gypsum, and magnesite shows promising results, especially bauxite and magnesite, which could lower As concentrations to below 0.1 $\mu\text{g/L}$. Both bauxite and magnesite worked efficiently on As removal even at higher concentrations above 5 mg/L , while gypsum is preferable for treatment of low As concentrations. Furthermore, magnesite has a unique chemical character of influencing other materials to have high efficiency of As removal; however, it raises the pH of the water up to 10. Addition of 5 g/L magnesite to water containing 5 mg/L As, could lower the As concentration to below 10 $\mu\text{g/L}$ within 30 min. The As removal increased with dosage and contact time up to 98 % in 4 hours, which is in agreement with Visual MINTEQ simulation. The performance of calcined magnesite, and gypsum fitted well with Freundlich adsorption isotherm, which indicates the presence of chemical reaction as controlling factor for As removal, while bauxite fitted Langmuir isotherm indicates monolayer surface coverage. The kinetic reactions were observed to follow pseudo-second-order. The statistic obeys linear regression with R^2 ranging between 0.7 and 0.9. The artificial neural network revealed pH as a most influencing parameter for As removal from water. The mini-scale column revealed that a flow rate of 0.5 – 1 mL/min for 30 min gave an adsorption capacity ranging between 0.07 and 0.14 $\mu\text{g/g}$, which follows Thomas linear model with rate constant of k_{TH} of 29.48 to 211.25 $\text{mL/min } \mu\text{g}$.

The release of elements from spent magnesite, gypsum, and bauxite, such as magnesium (Mg), aluminum (Al), iron (Fe), and calcium (Ca) were found to be below WHO standards after water treatment. However, the desorption process of As from spent magnesite and gypsum was a challenge, which means there was formation of strong bond between Mg-O-As and Ca-O-As.

This study is based on 5 papers that provide significant insights to the scientific community, policymakers, and the community living around As contaminated areas to learn about the occurrences of As and simple remediation techniques evaluated in this study.

Keywords: *Arsenic; bauxite; gypsum; magnesite; natural water; removal; Visual MINTEQ; kinetic reaction; isotherms; Freundlich; Langmuir.*

1. INTRODUCTION

Arsenic (As) is a toxic element which exists in the earth's crust (Duker *et al.*, 2005; Sadiq, 1997). It is a metalloid represented in the periodic table in group VA. The occurrence of As in the environment is through natural sources mobilized by rock weathering and sulfide minerals oxidation (Bhattacharya *et al.*, 2002). Human activities such as agricultural, industrial, and mining have contributed to As contamination in water bodies (Chang Chien *et al.*, 2012).

Arsenic exists in both inorganic and organic forms (Chang Chien *et al.*, 2012), of which organic forms are assumed to be less harmful and easily eliminated from the body through metabolic processes (Bhattacharya *et al.*, 2002; Kapaj *et al.*, 2006). In natural water, inorganic forms of As(III) and As(V) exist depending on the oxidizing and reducing environment (Gustafsson and Bhattacharya, 2007). Its speciation is controlled by pH, while its distribution is mostly controlled by redox potential. As(III) is known as more toxic since it forms a bond with sulfhydryl and thio groups of body proteins and can cause cell damage (Anand, 2022).

The main routes for As exposure for human beings are through drinking water, ingestion of food contaminated with As, and inhaling contaminated air (Chung *et al.*, 2014). The long-term exposure to this element will cause health problems such as (skin, kidney, liver, bladder) cancer and gangrene of the limbs, failure of internal organs, conjunctivitis, hyperkeratosis, hyper pigmentation, cardiovascular diseases, disorders of the central nervous system and peripheral vascular system (Kar *et al.*, 2011).

The drinking water guideline for As was set by the World Health Organization (WHO) to be 0.01 mg/L (WHO, 2017; Cotruvo, 2017). However, more than 200 million people in South Asian countries like Bangladesh, India, Pakistan, China, Nepal, Vietnam, Myanmar, Thailand, and Cambodia depend on arsenic (As) contaminated water sources (Yadav *et al.*, 2022). In Africa, the occurrence of natural As is reported in Ethiopia, West Africa, South Africa, and Tanzania, while anthropogenic sources were reported in Egypt, Ghana, Kenya, and South Africa (Irunde *et al.*, 2022).

Removal methods such as precipitation, ion exchange, reverse osmosis, nanomembrane, electrodialysis, and adsorption are useful to remove As from water (Irunde *et al.*, 2022). The reverse osmosis and electrodialysis methods are highly expensive to qualify for application in low-income countries. Thus, precipitation and adsorption processes are of interest due to their simple application and low operation costs.

Considering health problems caused by As and the contribution to the United Nations Sustainable Development Goals on safe, clean water, and sanitation for all (SDG6) under 6.1: safe and affordable drinking water, it is necessary to predict and prepare a simple method to remove As from water.

The current study presents the results obtained from water treatment with locally available mineral rock materials such as magnesite, bauxite, and gypsum. The parameters such as adsorbent dosage, pH, contact time, and initial As concentration were evaluated in batch experiments using natural water and a prepared spiked As solution in the laboratory. The mini-scale column was also conducted to evaluate flow rate and adsorption capacity.

2. AIMS, OBJECTIVES, AND RESEARCH QUESTIONS

2.1. RATIONALE

The As contamination of drinking water sources around Lake Victoria basin and gold mining areas of Geita and Mara in northern Tanzania is an alarming issue, which is associated with many patients admitted at the Ocean Road Cancer Institute being affected from cancer. The current study

evaluated locally available mineral rocks of bauxite, gypsum, and magnesite, which will be applied to design drinking water filters in rural areas of Geita and Mara.

2.2. OBJECTIVES AND RESEARCH QUESTIONS

2.2.1. General objective

The aim and objective of the present study were to evaluate simple methods that can be applied for As removal from water using bauxite, gypsum, and magnesite.

2.2.2. Specific objectives

Specific objectives were:

- To determine levels of arsenic from water samples around gold mining in Geita and Mara (*Paper I & II*).
- To determine mineralogical composition of the locally available mineral rocks of magnesite, bauxite, and gypsum (*Paper III, IV & V*), and
- To evaluate efficiency of magnesite, bauxite, and gypsum for As removal from water (*Papers III, IV & V*)

2.2.3. Research questions

The specific objectives were achieved through the following research questions:

- Are there water sources with As exceeding WHO guidelines in Geita and Mara?
- What are the major cations, anions, and As species in the water sample selected for As removal evaluation?
- What is the main composition of the mineral rocks, bauxite, gypsum, and magnesite?
- How much arsenic was removed from the water?
- How do the parameters contact time, initial As concentration, and pH influence As removal from water?
- What is the flow rate needed in the mini-scale column?

2.3. SCOPE OF THE STUDY

This study is limited to the application of locally available geogenic materials (minerals) bauxite, gypsum, and magnesite for batch experiments and min-scale column for Arsenic removal from drinking water. The water sample was collected from a source that was used for drinking, irrigation, and other household activities.

2.4. THESIS STRUCTURE

This thesis is divided into six main sections. Section 1 gives a general introduction and the background to the research problem. Section 2 explains the research problem and states the objectives and scope of the study. Section 3 is the background of the study. Section 4 describes the materials and methodology. Section 5 highlights the results. Section 6 is a discussion, while Section 7 is the conclusions and recommendations for future studies.

3. BACKGROUND

Although As has been known as a harmful element to humans exposed through drinking water, food, inhalation, and dermal contact (*Chung et al., 2014*), there is a knowledge gap in African countries such as Tanzania where As is not yet listed for water quality test for the drinking water.

Over a few years, As levels were reported to increase in water sources around gold mining areas under Lake Victoria basin in Tanzania (*Ligate et al., 2022*); however, the Government of the United

Republic of Tanzania (URI) has not taken strong initiatives for testing As. Limited studies have been conducted to reveal As contamination in water, soils, sediments, and vegetables as well as in urine (Nyanza *et al.*, 2014, 2019), and removal technologies have not yet been tested and or implemented, even in large gold mining areas of Geita and Mara.

3.1. MINING ACTIVITIES IN GEITA AND MARA

The large gold mining areas of Geita and Mara contribute economically to the mining sector of Tanzania. The large miners are careful to follow the rules and regulations that the Government of United Republic of Tanzania sets on environmental impact monitoring. However, artisanal and small-scale gold mining (ASM) activities are carried out in an uncontrolled manner in the Geita and Mara regions of northern Tanzania. Due to these small-scale mining operations, the government and mining sectors face difficulties in implementing policies and regulations that are required to ensure environmental as well as community safety (Kinyondo and Huggins, 2021). Most artisanal and small-scale miners have lower incomes, which limits them to attain all the processes that are required before mining the gold, such as environmental impact assessment, and they can cause severe damage to the land, soil, air, vegetation, and water systems. Some of the small-scale mining was reported to be conducted in hard to reach areas, with limited information to the government administration (Kinyondo and Huggins, 2021). Types of small-scale mining such as alluvial mining (along riverbanks), surface or subsurface mining, and hard rock mining can lead to changes in environmental morphology (geomorphological) and contribute to pollution in the water system. The geomorphological processes such as weathering of broken rocks, land sliding, soil erosion, effect on groundwater flow, and reduction of water table (Macháček, 2019) can accelerate chemical release into water systems.

A recent gender-based qualitative study (Leuenberger *et al.*, 2021) conducted in northwestern Tanzania reported how the community suffers negative impacts of mining, such as loss of agricultural land, house cracks from mining blasting, water pollution from mining chemicals, soil contamination, skin rashes, miscarriages, dust from the mining causing coughs and flu, intestinal diseases in children, early pregnancy in girls, Human Immunodeficient Virus (HIV) while the positive impacts were construction of new roads, water wells and health centers (Leuenberger *et al.*, 2021). Furthermore, other studies on dust exposure of mining workers reported high-risk respiratory diseases (such as phlegm, coughing, wheezing, breathless, and chest tightness) affecting the underground workers, exposed to a calculated geometric mean of $0.41 \pm 0.28 \text{ mg/m}^3$ compared to open pit workers with $0.17 \pm 0.23 \text{ mg/m}^3$, despite using protective equipment (Rusibamayila *et al.*, 2018).

For minimizing the poor public health and environmental degradation in artisanal and small mining sectors, the inclusiveness of the community in policymaking and its implementation is encouraged (Rwiza *et al.*, 2023). The formulation of mining laws should be bottom-up, with all people contribute ideas to policymaking. The scientific findings should be included in policymaking to ensure problems are solved (Rwiza *et al.*, 2023).

3.2. ARSENIC

The ability of As to bind with elements such as C, O and the =SH groups lead to toxicity in the human body. Arsenic (III) interferes with cell metabolic processes in the body and leads to cell damage when it bonds to thiol groups of proteins (Herath *et al.*, 2016).

3.2.1. Field measurements of Arsenic

Preliminary analysis in-situ is important to detect the presence of As. Thus, the test is performed through arsenic field test kit with color range between 0 and 500 $\mu\text{g/L}$. This technique shows ranges of As concentrations in the water samples.

Table 1 The principal techniques for As removal (Ahmad et al., 2017; Maity et al., 2021; Mohan and Pittman, 2007) (Paper I).

Methods	Technique	Advantage	Disadvantage
Oxidation/precipitation	Oxygenation	Simple in-situ As removal, low cost but slow	Removes arsenate and accelerates oxidation
	Chemical oxidation	Microbial disinfection, while oxidizes impurities, rapid process	Efficient control of pH and oxidation steps is required
Coagulation/coprecipitation	Alum coagulation	Low cost, simple operation, wide pH range application	Produces toxic sludge, low removal, peroxidation required
	Iron coagulation	More efficient than alum	Medium As(III) removal, sedimentation, and filtration required
	Lime softening	Availability of commercial chemicals	Readjustment of pH is required
Sorption and ion-exchange	Activated alumina	Commercially available	Need replacement after 4 to 5 regenerations.
	Iron coated sand	Cheap, no regeneration is required, remove both As (III) and As (V)	Not standardized; produces toxic waste
	Ion-exchange resin	Well defined medium and capacity, pH-independent, exclusive ion specific for As removal	High-cost medium, high-tech operation and maintenance, problem of concentrate disposal during regeneration, As (III) not removed
Membrane	Nanofiltration	High removal efficient	High capital and running costs
	Reverse osmosis	No toxic solid waste is produced	High tech operation and maintenance
	Electrodialysis	Capable to remove other contaminants	Toxic concentrate produced
Bioremediation	Bacteria, fungi, algae	Environment friendly	
	Plant accumulation	Green process, high efficient	Efficiency is affected by plant age and phosphate concentration

3.2.2 Laboratory measurements

The samples collected from the field or produced from an experiment are filtered, acidified with nitric acid, and stored in the refrigerator at 4°C for further analysis. The total arsenic concentrations are analyzed through inductively coupled plasma optical emission spectroscopy (ICP-OES) and inductively coupled plasma mass spectrometry (ICP-MS). Speciation of arsenic to show As(III), As(V), and organo-arsenicals is performed through high-performance liquid chromatography connected to inductively coupled plasma mass spectrometry (HPLC-ICP-MS). The major anions are usually analyzed through Ion chromatography (IC).

3.2.3. Arsenic removal techniques

Implementation of arsenic removal is very important to secure the society living around contaminated areas. The remediation techniques (Table 1), such as coagulation, precipitation, ion exchange, reverse osmosis, oxidation, adsorption, nanofiltration, electrodialysis, adsorption, and bioremediation through plants or bacteria, have been reported elsewhere (Ahmad *et al.*, 2017, 2019; Maity *et al.*, 2021).

The reverse osmosis and nano filter membranes (Table 1) are effective methods for As removal from water; however, the running costs are unmanageable in the lower income countries. Thus, the adsorption method from the application of locally available materials is more preferred for water treatment since its application is simple (Herath *et al.*, 2016).

3.3. FACTORS AFFECTING ARSENIC ADSORPTION EFFICIENCY

There are several factors that can influence or hinder As adsorption from water. Parameters such as initial As concentrations, adsorbent dosage, pH, and contact time are of importance for As uptake from water.

3.3.1. Initial As concentration

The initial As concentrations can inhibit As removal depending on the capability and porosity of the adsorbent. In previous studies, As adsorption was reported to decrease with an increase in As concentration (Chen *et al.*, 2016).

3.3.2. Adsorbent dosage

It was reported that an increase in adsorbent dosage increases As adsorption (Chen *et al.*, 2014). The As removal in the current study was increasing with dosage, and the uptake was low at low dosage (Irunde *et al.*, 2023).

3.3.3. pH

This is the parameter that has a major influence on metal and As speciation (Tahmasebpoor *et al.*, 2022). For magnesite materials, with a high point of zero charge (pHpzc) of more than 11, where the adsorption is favoured at higher pH above 11 (Masindi *et al.*, 2014). For materials with low pHpzc, such as bauxite, the adsorption decreases with an increase in pH following the Lewis adsorption process. The pH affects the surface charge of the adsorbent and makes the surface positively or negatively charged (Chen *et al.*, 2016).

3.3.4. Contact time

The longer the water is in contact with an adsorbent, the more the As adsorption (Chen *et al.*, 2014). Prolonged contact times in the current study were observed to improve the adsorption removal (Irunde *et al.*, 2023).

4. METHODS

The current study was carried out through field visiting observations, sample collection, laboratory analysis, and application of locally available materials (magnesite, bauxite, and gypsum) for As removal experiments.

4.1. STUDY AREA

The northwestern part of Tanzania around Lake Victoria Basin (LBV) is a well-known area for gold mining activities. The current study focuses on Geita and Mara gold mining areas (Fig. 1). The main gold mining areas are Geita Gold Mining (GGM), with latitude -2.8333°, longitude 32.1667°, and North Mara Gold Mining (NMGM) with latitude -1.4667°, longitude 34.5167°. Geita region

border the south shores of Lake Victoria, while the Mara region is in the Eastern part of Lake Victoria. The geology of Geita and Mara consists of Archean granitoid-greenstone belts enriched with gold deposition through sulfide minerals such as pyrite and arsenopyrite. The greenstone belt is covered by granitic, gneissic, and migmatitic rocks cover the greenstone belt. The continuous evolution of the greenstone belt around gold mining area in northern Tanzania has led to formation of lithologies such as felsic volcanic, ferruginous rocks, and metasediments. The population around the area is estimated to increase every month due to mining activities. The indigenous population is involved in agricultural, fishing, and grazing animals and livestock. Due to climate change impacts, animal keeping has been declining with time since the farmers are forced to reduce number of cows due to lack of pasture.

The area is characterized by high lands (hills), low open land, and wetlands with sedimentary rocks underneath. The soil in the area contains organic matter that supports vegetation growth around the area. Because of the vegetation cover, the presence of bacteria around the area for nitrate fixation is expected. The presence of microbes under the vegetation cover contributes to economic activities such as the biotransformation of contaminants in the area. Some bacteria survive at low pH and in reducing environments and are expected to introduce the dissolution of arsenic bound to iron oxide. Furthermore, bacteria that survive in an oxidizing environment tend to oxidize sulfide minerals and release arsenic into the water system. Bacterial use arsenic for energy metabolism. The presence of bacteria that affect arsenic behavior was observed when an acidified water sample collected from Geita and Mara submitted to the laboratory showed less arsenic compared to the amount tested in the field. This indicates that bacteria could utilize most of the arsenic during transportation from the field to the laboratory.

4.2. COLLECTION OF WATER SAMPLES AND THE LOCAL ADSORBENTS

4.2.1. Collection of water samples

The water samples were collected during a field campaign around the mining areas of Geita and Mara from different periods between 2016 and 2019. The water samples in Geita and Mara were sourced from shallow wells, deep wells, bore holes, spring streams, river streams, and rainwater. To a 1 litre plastic bottle, cleaned with nitric acid and rinsed with distilled water, the filtered water sample was introduced and capped.

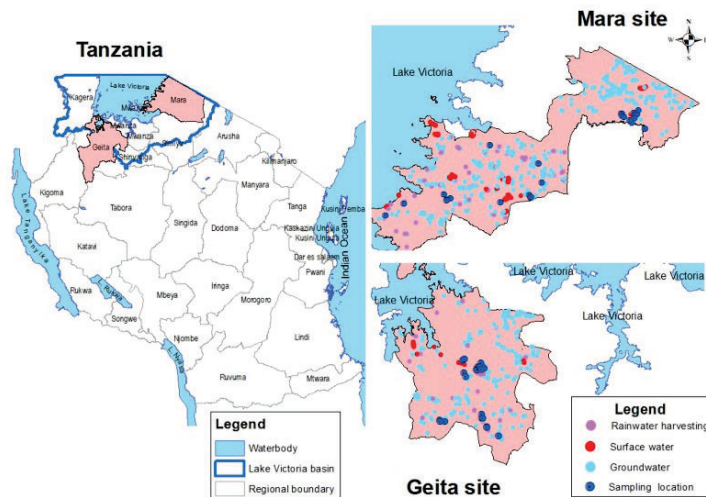


Figure 1. Study area for water sampling around Geita and Mara, northern Tanzania.

During water sampling, several parameters were observed in the field, such as color of the water, odour, pH, electroconductivity, temperature, arsenic level by using arsenic test kit, and redox potential. Besides, rock samples from wells were collected for further investigation of what might be the source of arsenic around Geita and Mara gold mining basin.

4.2.2. Collection of local adsorbents bauxite, gypsum, and magnesite

The locally available materials are distributed all-over Tanzania from the north to southern part. However, the presented materials in the current study were collected from bulk deposits of Moshi-Makanya (gypsum), Lushoto-kwemashai (bauxite), and Moshi-Chambogho (magnesite). The mentioned areas are large mining areas for bauxite, gypsum, and magnesite and contain bulk reserves that can last for decades.

4.2.3. Sample treatment and analysis

The water samples of 1 litre each were filtered in the field through 0.45 μm membrane and acidified with 2% nitric acid, capped, and packed in iceboxes ready for transportation to the water laboratory at the University of Dar es Salaam. Thereafter, water samples were kept in a fridge at 4 °C until the analysis time using ICP-OES, IC, to characterize major cations and anions.

Some samples were sent to the Tanzania bureau of standards (TBS) Tanzania Chemistry Lab (GCA), and some were transported to Sweden to the SEED lab, and ALS to investigate arsenic species by using HPLC-ICP-MS.

Rock samples collected from Geita and Mara were sent for petrographic analysis at the Geology Department, University of Dar es Salaam, to investigate the mineralogical characteristics around Geita and Mara.

4.2.4. Preparation of adsorbent materials

The local rock materials were brushed clean, washed, dried, crushed into powder form, and calcined at temperature of 500 °C. This temperature was reported to be effective for bauxite calcination (Mohapatra, 2008). The calcination time was set to 2 hours to save energy consumption during future production. After calcination, the samples were stored in plastic containers ready for application in water treatment for arsenic removal.

The calcined samples were characterized to investigate mineralogy content by using X-ray diffraction (XRD), BET, and SEM, as described below, and digested mineral samples were checked by ICP-OES.

A portion of raw and calcined (bauxite, gypsum, and magnesite) powder sample was inoculated on the X-ray diffraction (XRD) sample-plate and placed in the Panalytical Xpert Pro X-ray diffractometer (Cu-K-alpha1). The scan range (2θ) of diffractometer was 10 – 80 degrees within 15 minutes (40 mA, 45kV). The obtained XRD diffraction data were analysed in X'Pert High-Score software under the database from International Center for diffraction data (ICDP PDF-4+ 2022) to identify mineral phases that exist in the local materials of bauxite, gypsum, and magnesite sample. Portions of powder samples were introduced in JEOL field emission scanning electron microscope (FE-SEM-EDS, JSM-7000F) to determine the elemental composition and the morphology of the local material. Furthermore, the surface area of the material was analyzed using the Brunauer Emmett Teller (BET) method under adsorptive nitrogen (N_2) and an equilibration interval of 15 seconds.

The content of iron (Fe) and As in the raw material was investigated by digesting 5 g material in 10 mL concentrated nitric acid, heated at 115 °C for 2 hours. The filtrate was diluted with distilled water to 100 mL and measured with inductively coupled plasma atomic emission spectroscopy (ICP-OES, iCAP 7600).

4.3. WATER TREATMENT FOR ARSENIC REMOVAL

The water sample collected from Masinki stream at latitude -1.48672° , longitude 34.50887° , elevation 1198 m in Tarime in Mara district was used in a batch experiment to evaluate As removal through application of bauxite, gypsum, and magnesite separately. About 100 g/L of adsorbent was poured into the As solution and shaken vigorously for 4 hours at 70 rpm while 10 mL aliquots were taken at intervals of 10 to 20 minutes. The samples were filtered through 0.45 μm filter, acidified, and sent to the specific laboratory for arsenic analysis.

For higher arsenic concentration removal, synthetic (spiked distilled water) water containing arsenate was prepared at the SEED laboratory and applied in batch experiment for the As removal. A stock solution of 100 mg/L $\text{Na}_2\text{HAsO}_4 \cdot 7\text{H}_2\text{O}$ was prepared to be used for dilution to prepare lower initial As concentrations such as 0.1 mg/L, 0.5 mg/L, 1 mg/L, 3 mg/L, 5 mg/L, and 10 mg/L up to 30 mg/L at near neutral pH. The amount of bauxite, gypsum, and magnesite was poured into the water sample containing the mentioned concentrations above and agitated vigorously at room temperature. The parameters of interest on how they affect arsenic removal, such as contact time, pH, adsorbent dosage, and initial concentration, were evaluated through linear regression and neural networks in SPSS version 28.

4.3.1. Bauxite (Paper IV)

The pH of the raw and calcined bauxite material was investigated by shaking 2 g per 10 mL distilled water with initial pH 1.51, 1.73, 2.26, 2.31, 2.46, and 4.2. The As removal procedure using raw, calcined, and alkaline ferric-bauxite composite was evaluated.

4.3.1.1. Raw bauxite

In the 1 mg/L As water at pH 7, 100 g/L of raw bauxite was introduced and shaken at 70 revolutions per minute (rpm) for 4 hours while water samples were collected at 20 minutes intervals.

4.3.1.2. Calcined bauxite

0.5 g/L, 5 g/L, or 50 g/L calcined bauxite was introduced in the solution of 5.3 mg/L As, shaken vigorously at 70 rpm. In natural water, 100 g/L calcined bauxite was introduced in water contain 117 $\mu\text{g/L}$ and 5.3 $\mu\text{g/L}$, shaken vigorously. The samples collected were filtered through a 0.45 syringe filter and stored in a fridge at 4 $^{\circ}\text{C}$ ready for analysis in ICP-OES. The high dosage of 100 g/L of calcined bauxite was introduced in the As solution of 1 mg/L at pH 7, shaken for 4 hours, and sample was collected at 20 minutes intervals. The pH was slightly raised above pH 7 since the bauxite was heated in the furnace in the presence of magnesite, which might absorb carbon dioxide emitted from magnesite. Bauxite was also newly crushed and heated in the furnace in the absence of magnesite since the previous was slightly raising pH, and 5 g/L was shaken in 5.3 mg/L As water to evaluate pH effect.

4.3.1.3. Alkaline ferric-bauxite composite

The 50 g raw bauxite powder was poured into 100 mL of 0.5 M ferric nitrate, and the pH was raised by 0.1M NaOH up to pH 12. The mixture was shaken for 12 hours at 75 $^{\circ}\text{C}$ under 250 rpm. After 12 hours, the composite was dried at 105 $^{\circ}\text{C}$ for 24 hours and kept in a dry container. This composite had high pH to investigate if As is enhanced at high pH. For batch experiment, 5 g/L of ferric-bauxite alkaline composite was poured into 2 mg/L As water at initial pH 4.

4.3.1.4. Arsenic solution

The desirable arsenic solution of different concentrations was prepared from stock of 100 mg/L $\text{Na}_2\text{HAsO}_4 \cdot 7\text{H}_2\text{O}$ for removal evaluation. The initial As concentrations of 0.1, 0.5, 1, 2, 5, 10, 15, 20 and 30 mg/L were prepared from stock solution of 100 mg/L. The initial pH was regulated by 0.1M NaOH and nitric acid. The bauxite amount of 0.5 g/L, 5 g/L, 50 g/L, and 100 g/L were introduced into the solution, shaken, filtered, and analyzed using ICP-OES.

4.3.1.5. Leaching tests

Leaching of As from 1g calcined bauxite waste used for water treatment to reduce the concentration of 10 mg/L to 0.0018 mg/L As, was accomplished through mixing the material with 10 mL of 0.1 M NaOH, shaken vigorously for two hours, filtered, and analyzed using ICP-OES.

4.3.2 Gypsum (Paper V)

The As water solutions of different initial concentrations of 0.5, 1, 3, 5, and 10 mg/L were prepared by dilution of 100 mg/L $\text{Na}_2\text{HAsO}_4 \cdot 7\text{H}_2\text{O}$ stock solution. The pH tests of the gypsum were preliminarily investigated by shaking distilled water with 100 g/L raw gypsum at initial pH 4.2 and pH 1.51.

To the small bottles with 5.266 mg/L As solution of pH 7, the 50 g/L and 100 g/L gypsum were introduced and shaken at 70 rpm for three to five hours. In the natural water from the field with 117 $\mu\text{g/L}$ As(V) and 5.3 $\mu\text{g/L}$ As(III) (Irunde *et al.*, 2023), the 100 g/L of calcined gypsum was poured and shaken vigorously. The samples were taken at intervals of 30 minutes, filtered through 0.45 μm , acidified with nitric acid, and kept in a fridge at 4 °C ready for the analysis in inductively coupled plasma atomic emission spectroscopy (ICP-OES, iCAP 6000). The ICP-OES was calibrated using the multielement standard solution to the R^2 of 0.99, and the calculated relative standard deviation of the most As concentration results were below 0.9%.

The cations and anions from natural water samples were simulated through a geochemical software, Visual MINTEQ, version 3.1 (Gustafsson, 2022), to understand the As removal trend and evaluation of saturation indexes. Visual MINTEQ is a geochemical model that is used to simulate metal speciation from water, the saturation index of metals, complexation of metals onto surface, and toxicity measures. The importance of parameters was evaluated using linear regression and artificial neural networks from SPSS version 28.

4.3.2.1. Desorption of As from spent gypsum

The leaching of 1 mg/L As from the application of 50 g/L spent calcined gypsum was carried out using 1 g spent gypsum, poured in 10 mL of 0.1 M NaOH, shaken vigorously for two hours, filtered, and analysed in ICP-OES.

4.3.3 Magnesite (Paper III)

Arsenic solutions were prepared through dilution of the stock As solution of 100 mg/L $\text{Na}_2\text{HAsO}_4 \cdot 7\text{H}_2\text{O}$. The initial As concentrations prepared at near neutral pH varied from 0.1, 0.5, 1, 2, 3, 5, and 10 mg/L for kinetic studies to determine equilibrium time, equilibrium concentration, equilibrium capacity, and the effect of initial concentration on As removal. In the As(V) solution, 0.5 g/L, 5 g/L, and 50 g/L magnesite were introduced and agitated vigorously at 70 rpm at different times such as 2 min, 5 min, 15 min up to 4 hours. For the natural water sample, 100 g/L was shaken vigorously with 117 $\mu\text{g/L}$ As(V) and 5.3 $\mu\text{g/L}$ As(III). The samples were filtered through 0.45 μm filter and kept in a fridge at 4 °C for the subsequent analyses. The samples with pH higher than 10 and above were acidified using 20% nitric acid. The quality check from sampling to instrumental analysis was considered to minimize errors from measurements. Analytical instruments, such as ICP-OES, were calibrated using analytical grade multi-standard solutions, and the calibration model fit was recorded at $R^2 = 0.99$. For ICP-OES, the standard solution run was repeated after 8 samples to correct the instrument drift. The average of triplicate measurements was reported, and the relative standard deviation was less than $\pm 5\%$.

To determine the best calcined magnesite dosage, the amount in concentration was varied from 0.05 g/L, 0.5 g/L, 5 g/L, 50 g/L, and 100 g/L and shaken with As solution at near neutral initial pHs. Preliminary pH tests in this study involved 200 g/L calcined magnesite at initial pH of 1.51 since pH 4.2 and 2.3 raised pH above 10.

4.3.3.1. Leaching of As from spent magnesite

Extraction of As from calcined magnesite was evaluated using 10 mL of 0.1 M NaOH introduced in a bottle containing 1 g of spent material and shaken vigorously for two hours.

4.4. MINI-SCALE COLUMN EXPERIMENT

The four mini-scale columns (see Fig. 36) packed with 20 g of 1 mm calcined locally available materials were used to evaluate flow rate (Table 8) and the effluent levels of As concentrations at 30 min (Table 7). The water sample was collected from Botanga bore hall in Matongo, Mara. The inlet plastic container of 5 litres filled with natural water was placed 70 cm high to allow water flow by gravity into the 20 cm long mini-scale column with diameter of 1.92 cm (perfluoroalkoxy tubing) connected to 0.4 cm plastic inlet tubes. The column was supported with 5 g clean sand at the inlet and 3 g at the outlet. The sand was acid washed, cleaned with plenty of water, then boiled with hot water at 100 °C for two hours, rinsed, and dried at 105 °C for 24 hours.

Column 1 was packed with 20 g magnesite, supported with 5 g washed sand at the inlet and 3 g washed sand at the outlet, while column 2 was packed with 20 g bauxite supported with 5 g washed sand at the inlet. The column 3 was packed with 20 g gypsum supported with 5 g washed sand at the inlet and 3 g washed sand at the outlet. The column 4 was packed with the ratio of 1:1:2, which means 5 g of magnesite, 5 g of gypsum, and 10 g of bauxite signified as BGM filter. The reason for packing 10 g bauxite near the outlet in column 4 was to enhance pH regulation, as it was hypothesized in the DAFWAT project that bauxite lowers pH.

4.5. THEORETICAL CALCULATIONS

There are several simple formulas that were applied to prepare solutions and to fit the experimental results from this study.

Arsenic stock solution preparation from the salt $\text{Na}_2\text{HAsO}_4 \cdot 7\text{H}_2\text{O}$ where the molecular for As itself is 75 g/mol and the required stock solution is 100 mg/L in 200 mL, therefore:

$$\text{Weight of As (wt) (g)} = \text{Molarity of As (Mr}_{\text{As}}) \times \text{total molecular weight of the salt (M.W. total)} \times \text{volume (L)} \quad (\text{Eqn. 1})$$

The dilution law is applied to prepare lower concentrations from stock solution.

$$\text{Molarity of concentrated solution (Mc)} \times \text{Volume of concentrated (Vc)} = \text{Molarity of diluted solution (Md)} \times \text{Volume of diluted solution (Vd)} \quad (\text{Eqn. 2})$$

Preparation of a nitric acid solution from a concentrated acid

$$\text{Mc Nitric acid} = [\text{density } (\delta) \text{ of the concentrated solution} \times \text{percentage by weight (wt}\% \text{)} \times 1000] / \text{molecular weight (M.W)} \quad (\text{Eqn. 3})$$

Equation 3 helped to calculate how much volume (in mL) can be taken from the commercial nitric acid bottle and to be diluted to get the required concentration in moles. The density, *i.e.* percentage by weight and molecular weight are listed on the bottle containing concentrated nitric acid.

The percentage removal was calculated as

$$\% \text{ Metal removal} = [\text{Initial metal concentration (C}_0\text{)} - \text{final metal concentration (C}_f\text{)}] / \text{C}_0 \times 100 \quad (\text{Eqn. 4})$$

The mass balance or removal capacity (qt) was calculated from

$$\text{qt} = ((\text{C}_0 - \text{C}_t) \text{ V}) / \text{mass (g)} \quad (\text{Eqn. 5})$$

The saturation index (SI) of mineral precipitates from geochemical models were calculated from

$$\text{SI} = \text{Log} [\text{Ion Activity Product (IAP)} / \text{solubility constant (Ks)}] \quad (\text{Eqn. 6})$$

SI = 0 signifies the minerals are at equilibrium, while SI>0 signifies formation of mineral precipitate in the water, and SI<0 signifies the minerals are dissolved in the solution.

The simple linear regression model helped to determine relationship between parameters, such as initial concentration, pH, contact time, and dosage (Irunde *et al.*, 2023).

$$y = ax + c + \epsilon \quad (\text{Eqn. 7})$$

where y axis is dependent variable, “a” is a slope, x is independent variable, c is constant, and ϵ is standard error.

For chemical reactions, rate law orders, half-life (Irunde *et al.*, 2023; Mata-Perez and Perez-Benito, 1987), pseudo-second order, adsorption isotherms, and thermodynamic calculations, the following simple equations (Irunde *et al.*, 2023; Masindi and Gitari, 2016; Mata-Perez and Perez-Benito, 1987; Mohapatra *et al.*, 2008)(Salje, 1988) were used in *Papers III, IV, and V*.

Zero order rate law (Eqn. 8) and its half-life ($t_{1/2}$) (Eqn. 9) where k is the rate constant.

$$C_f = -kt + C_0 \quad (\text{Eqn. 8})$$

$$t_{1/2} = \frac{C_0}{2k} \quad (\text{Eqn. 9})$$

First order rate law (Eqn. 10) and its half-life (Eqn. 11)

$$\ln C_f = -kt + \ln C_0 \quad (\text{Eqn. 10})$$

$$t_{1/2} = \frac{\ln 2}{k} \quad (\text{Eqn. 11})$$

Second-order rate law (Eqn. 12) and its half-life (Eqn. 13)

$$\frac{1}{C_f} = kt + \frac{1}{C_0} \quad (\text{Eqn. 12})$$

$$t_{1/2} = \frac{1}{kC_0} \quad (\text{Eqn. 13})$$

Pseudo-second order (Eqn. 14) where t is time in minutes, q_t and q_e are adsorption capacity (mg/g), k_2 is a rate constant of the pseudo-second order.

$$\frac{t}{q_t} = \frac{1}{k_2 q_e^2} + \frac{t}{q_e} \quad (\text{Eqn. 14})$$

The rate constant for intraparticle diffusion (K_{id}) (Eqn. 15) is given by Weber Morris (Bulut *et al.*, 2007)

$$q_t = K_{id} t^{1/2} + C \quad (\text{Eqn. 15})$$

where C is the intercept.

In the Langmuir isotherm (Eqn 16), the linear equation below was fitted; where C_e is a concentration at equilibrium (mg/L), q_e amount adsorbed at equilibrium (mg/g), b the Langmuir constant (L/mg) related to the affinity of the adsorption sites, q_m is the maximum adsorption capacity (mg/g).

$$\frac{C_e}{q_e} = \frac{1}{b q_m} + \frac{1}{q_m} C_e \quad (\text{Eqn. 16})$$

To test if the Langmuir isotherm is favorable or unfavourable, a dimension-less constant separation factor, R_L (Eqn. 17), is applied, where C_0 is an initial concentration of As (mg/L).

$$R_L = \frac{1}{1 + bC_0} \quad (\text{Eqn. 17})$$

The nature of the adsorption process may be either unfavorable ($R_L > 1$), linear ($R_L = 1$), favorable ($0 < R_L < 1$) and irreversible ($R_L = 0$)

Thermodynamic function in Langmuir is presented in Equation 18.

$$\ln\left(\frac{1}{b}\right) = \frac{\Delta G}{RT} \quad (\text{Eqn. 18})$$

where $T = 291$ K, $b = 0.9594$ L/mg, $R = 8.3145$ J/mol/K

Freundlich reaction isotherm (Eqn. 19) describes the heterogenous surface of the adsorbent.

$$q_e = K_f C_e^{\frac{1}{n}} \quad (\text{Eqn. 19})$$

Equation 19 may be linearized by taking the logarithm of both sides of equation to form Equation 20.

$$\log q_e = \frac{1}{n} \log C_e + \log K_f \quad (\text{Eqn. 20})$$

where C_e is equilibrium concentration (mg/L), q_e is amount removed at equilibrium (mg/g), K_f is partition coefficient (mg/g), and “n” is intensity of removal.

The linear plot of $\log q_e$ versus $\log C_e$ indicates if the data is described by Freundlich reaction isotherm.

The value of K_f implies that the energy of contaminant removal on a homogeneous surface is independent of surface coverage, and “n” is an adsorption constant, which reveals the rate at which removal is taking place. These two constants are determined from the slope and intercept of the plot of each other.

The D-R isotherm model (Eqn. 21) is important to understand the type of removal mechanism by plotting the graph of $\ln C_e$ against \mathcal{E}^2 (Eqn. 21, 22 and 23) and calculating the sorption energy E_s , which is correlated with “k” (isotherm constant) (Bakatula *et al.*, 2017).

$$\ln C_e = \ln q_m - k\mathcal{E}^2 \quad (\text{Eqn. 21})$$

Where q_m is the maximum sorption capacity of sorbent (mg/g), \mathcal{E} is the Polanyi potential, R is the gas law constant 8.3145 kJ/mol K, T is the absolute temperature K,

$$\mathcal{E} = RT \ln \left[\left(1 + \frac{1}{C_e} \right) \right] \quad (\text{Eqn. 22})$$

$$E_s = \frac{1}{\sqrt{-2 \times k}} \quad (\text{Eqn. 23})$$

If the E_s is less than 8 kJ/mol, the process of adsorption is physisorption (ion-ion attraction). When E_s is between 8 and 16 kJ/mol, the process of adsorption is ion-exchange, but for E_s greater than 16 kJ/mol, the process of adsorption is chemisorption involving the formation of covalent bonds (Bakatula *et al.*, 2017).

From the Freundlich straight line equation, the k_f can help to calculate the free energy change ΔG° of the sorption for both anions using Eqn. 24.

$$\Delta G^\circ = -RT \ln(k_f \times 1000) \quad (\text{Eqn. 24})$$

where R is the gas constant (0.00831447 kJ/Kmol) and T is the temperature in Kelvin. The negative free energy signifies the feasibility of the process and the spontaneous adsorption (Chiban *et al.*, 2011).

In Thomas kinetic model, the linear form applied in column evaluation (Roy *et al.*, 2013) is represented as;

$$\text{Flow rate (Q)} \times \ln \left(\frac{C_o}{C_t} - 1 \right) = (k_{TH} \times q_t \times M) - (k_{TH} \times C_o \times V_{\text{outlet}}) \quad (\text{Eqn. 25})$$

where k_{TH} is the Thomas rate constant (mL./min \times μ g), q_t adsorption capacity of the column μ g/g, M is the amount of the adsorbent in the column, V_{outlet} the effluent volume (L), C_o is the inlet concentration (μ g/L), C_t is the effluent concentration (μ g/L).

5. RESULTS

5.1. ARSENIC OCCURRENCE AND CONTAMINATION IN THE ENVIRONMENT (*PAPERS I & II*)

This section briefly describes As contamination as a global challenge due to its toxicity and mobilization in the environment.

5.1.1 Occurrence (*Paper I*)

Arsenic occurs naturally from weathering of parent rocks bearing sulfide minerals through oxidation, dissolution, volcanic eruption, and thermal springs (Abiye and Bhattacharya, 2019; Bhattacharya *et al.*, 2002; Bundschuh *et al.*, 2013; Maity *et al.*, 2011; Nriagu *et al.*, 2007) Furthermore, climatic change factors such as drought or flooding can influence the mobilization of As in the environment (Irunde *et al.*, 2022). Human-induced pollution from industrial, mining, and agricultural activities has been contributing to the detrimental distribution of As in the soil, water, air, and vegetation (Bhattacharya *et al.*, 2010; Herath *et al.*, 2016; Irunde *et al.*, 2022).

For Africa, As is reported around the northern Egyptian delta lake associated with pesticides containing As and industrial wastewater flows (El-Badry and Khalifa, 2017). The natural occurrence of As related to the oxidation of sulfide minerals in agricultural and industrial applications of As in South Africa has been previously reported (Abiye and Bhattacharya, 2019). In West Africa, the occurrence of As was associated with the presence of gold deposits (Gbogbo *et al.*, 2017) and industrial activities (Asante *et al.*, 2012). In the semi-arid regions of West Africa, As are due to the geogenic oxidation of sulfide minerals in auriferous zones of volcano-sedimentary schists and volcanic rocks of Birimian formation influence As mobilization (Bretzler *et al.*, 2019).

The weathering of fluvial-volcano-lacustrine rocks hydrothermal water associated with high pH geochemical environment was reported to influence As mobilization in the East of the main Ethiopian Rift (Rango *et al.*, 2010, 2013). The oxidation of arsenopyrite in mine wastes and tailings was hypothesized to lead to As occurrence in Tanzania and Kenya (Kassenga & Mato, 2008; Nyanza *et al.*, 2014; Ogola *et al.*, 2002; Yang *et al.*, 2017). The concentrations of As were found close to the WHO drinking water guideline, except in some hotspots both in shallow groundwater and surface water sources in areas in close proximity to the gold mining activities in northern Tanzania. The concentration of As ranged between 1 and 300 μ g/L, and nearly 53% of all analyzed samples exceeded the WHO guideline value of 10 μ g/L (*Paper I*).

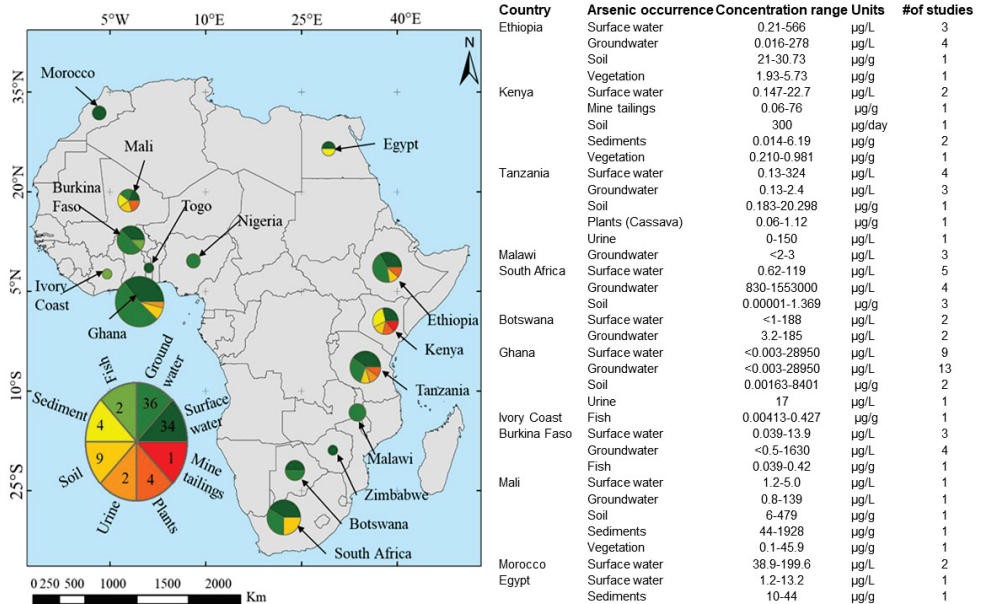


Figure 2. Arsenic occurrences and spatial distribution in Africa (Trunde et al., 2022).

The limited studies of As in Africa revealed information that it was spatially distributed among water systems, soils, sediments, vegetables, and fish (Fig. 2, Paper I). For the surface water, 30% of the minimum values exceeded 10 µg/L, one value of which was recorded in eastern Africa (Tanzania), the rest were recorded in western Africa, in Ghana (50%), Morocco (25%), and Togo (12.5%). Of the maximum values, around 74% were above 10 µg/L and were spatially distributed in northern (4.3%), southern (13%), eastern (26%), and western (57%) parts of Africa. In the northern part of Africa, this value was reported in Egypt, while the rest were reported in Zimbabwe (33.3%), South Africa (33.3%), and Botswana (33.5%) in southern Africa. In eastern Africa, the maximum values exceeding 10 µg/L were reported in Kenya (16.7%), Ethiopia (33.3%), and Tanzania (50%). In western Africa, these values were reported in Cote d'Ivoire (7.7%), Togo (7.7%), Morocco (15.5%), and Ghana (69.2%).

Furthermore, about 24% of groundwater samples exhibited the minimum As concentration exceeding 10 µg/L and were spatially distributed in eastern (14.3%), western (28.6%), and southern (57.1%) parts of Africa. In eastern Africa, As exceeding 10 µg/L was reported in Ethiopia while others were reported in Nigeria and Ghana within western Africa. More than 10 µg/L of As was reported in Botswana (25%), where 75% of the sample was observed in South Africa. For the maximum value, around 86% of the samples were reported to have As concentration above 10 µg/L and were spatially distributed in eastern (16.7%), southern (23.3%), and western (60%) parts of Africa. In eastern part, As values were reported in parts of Tanzania (20%) and Ethiopia (80%), while then reported in Botswana (28.6%) and South Africa (71.4%) in southern part of Africa. Likewise, these values were reported in parts of Nigeria (5.6%) and Mali (5.6%), Burkina Faso (22.2%), and Ghana (66.7%) in western part of Africa.

5.2. EVALUATION OF WATER SAMPLE CHARACTERISTICS IN GEITA AND MARA (PAPER II)

In Paper II, the physical and chemical characteristics of the water sample are described using different analytical and statistical analyses to understand the water chemistry in the environment.

Table 2. Results from 40 samples in Geita and Mara.

Area	As total µg/L	As(V) µg/L	As(III) µg/L	Al µg/L	Fe µg/L	Si mg/L	Ca mg/L	Sulfate mg/L
Geita-rural	100	36.7	2	2047.6	6312.8	30.28	76.7	5.29
Geita-Katariyo	100	56.3	3.19	30.8	0.29	14.7	46.5	45.3
Tarime-Kemambo	150	37.9	3.18	668.6	273.9	18	32	110
Tarime-Matongo	300	19.34	2	1602	961	20.6	35.6	
Tarime-Matongo	20	18.2		10	7.97	28.7	85	56.9
Tarime-Matongo	220	18.1	3	77	36	11.8	54	15.7

Paper II forms the foundation for the present study on As removal since it provided broad information on the more contaminated sites within Geita and Mara. From **Table 2** above, the presence of aluminium (Al), calcium (Ca), iron (Fe), silicon (Si), as well as sulphate reveals the existence of the natural factors that cause As contamination in water. The natural phenomena, such as the dissolution of Al/Fe hydroxide and oxidation of sulfide containing minerals, cause As level to increase in water (Ligate *et al.*, 2022).

The visual MINTEQ simulation of cations and anions present in the water samples in Geita and Mara was described in **Paper II** (Faneul *et al.*, 2022). The saturation indexes (Fig. 3) reveal whether a compound will precipitate in the natural water or dissolve, depending on whether the index is above zero or below zero (Ligate *et al.*, 2022). The information obtained from visual MINTEQ was useful for the preparation of removal technologies that are described in **Papers III, IV, and V**.

5.3. REMOVAL TECHNOLOGIES USING BAUXITE, GYPSUM, AND MAGNESITE (**PAPERS III, IV & V**)

The evaluated simple removal methods using locally available materials bauxite, gypsum, and magnesite are of importance due to their availability and ease of application. These materials show

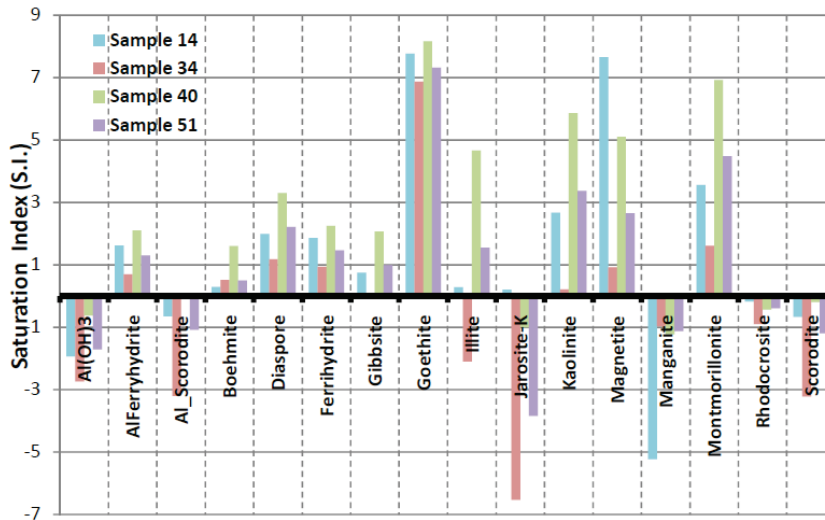


Figure 3. Visual MINTEQ saturation indices from cations and anions in water sources around Geita and Mara (Ligate *et al.*, 2022)

good trends of arsenic removal from water. Locally available materials, such as magnesite and gypsum, can also be applied to mining soil waste to capture As and form precipitates which are stable up to pH 12 (Sun *et al.*, 2022).

5.3.1 Magnesite (Paper III)

5.3.1.1. Characterization of magnesite

The X-ray diffraction data indicated that the raw magnesite contained magnesium carbonate (MgCO_3) as the main phase (Fig. 4), while the other phases were magnesium iron carbonate, siderite, and silicon dioxide (Irunde *et al.*, 2023). These phases (MgCO_3 , MgFeCO_3 , FeCO_3 , SiO_2) were also observed in calcined magnesite.

The MgCO_3 showed peaks positioned between 32.8° and 77° (Fig. 4) (Irunde *et al.*, 2023). The calcination process led to the formation of oxides, MgO , which was identified by peaks at 2θ of 21° , 43° , and 62° while Fe_2O_3 was identified by peaks between 32.8° and 70.5° (Irunde *et al.*, 2023). The peak overlapping was observed when more than one phase shared one peak (Fig. 4).

The field emission scanning electron microscope FE-SEM-EDS revealed the presence of high amount of oxygen (O), followed by magnesium (Mg), carbon (C), silicon (Si), Iron (Fe), and calcium (Ca), which confirms the sample is magnesite. The 5 g raw magnesite dissolved in 10 mL nitric acid under heating and later diluted to 100 mL was revealed to contain 87.48 mg/L Fe (Irunde *et al.*, 2023), which indicates the presence of iron compounds similar to siderite (FeCO_3). The calcination of magnesite increased the surface area to about 4 times; however, the pore size was slightly reduced (Irunde *et al.*, 2023).

5.3.1.2. Batch experiment

The calcined magnesite was observed to absorb more water to about 40% (Irunde *et al.*, 2023), which means significant loss of water molecules during heating at 500°C . The possibility of the magnesite to lose water under heating was previously studied in thermographic analysis (TGA) (Liang *et al.*, 2022; Natsi *et al.*, 2023).

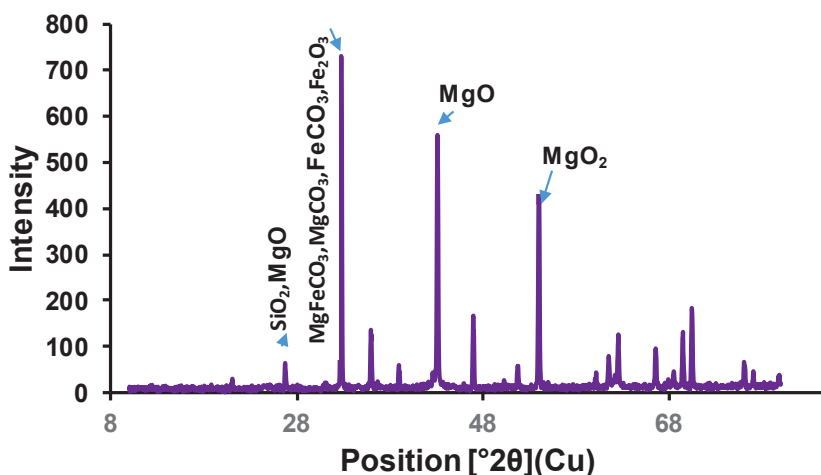


Figure 4. X-ray diffraction showing phases in calcined magnesite (Irunde *et al.*, 2023).

5.3.1.3. Natural water for As removal

The presence of cations and anions in the natural water sample, which was simulated in Visual MINTEQ 31 revealed that the chemical removal was increased with an increase in the adsorbent dosage (Fig. 5). There was rapid increase in removal to 99% when adsorbent dosage of 0.03 g/L was applied.

The cations and anions removal from natural water in the simulation was also influenced by pH (Irunde *et al.*, 2023). The pH 4 favored undersaturation, while the saturation index increased from pH 6.8 to 10. The precipitated compounds at pH 10, such as brucite, calcite, hydromagnesite, magnesite, $\text{MgCO}_3 \cdot 5\text{H}_2\text{O}$, and Nesquehonite might have contributed to chemical removal of As from water.

Arsenic speciation from the water sample revealed an oxidizing environment due to the presence of high As(V) and low As(III) in which, after treatment with 10 g/mL of calcined magnesite removed 99% As(V) and 98% As(III).

5.3.1.4. Synthetic (spiked) arsenic solution

The arsenic solution was prepared in the laboratory to evaluate the removal efficiency by calcined magnesite. The selected dosage was 0.05 g/L, 0.5 g/L, 5 g/L, 50 g/L, and 100 g/L, which were introduced to arsenic solution with initial concentrations ranging from 0.1 mg/L to 20 mg/L. The parameters such as initial concentration, contact time, dosage, and pH effects are reported below as how they affect removal percentage and removal capacity.

5.3.1.5. Initial arsenic concentration effect

The percentage removal was observed to decrease with an increase in initial As concentration from 0.1 mg/L to 20 mg/L when 0.5 g/L calcined magnesite was applied (Fig. 6). The decrease in removal as the effect of an increase in As initial concentration was in agreement with the previous study (Masindi *et al.*, 2014). For the higher dosage of 5 g/L, and 50 g/L, the removal percentage was observed to increase with the initial As concentration (Fig. 7). The 99% was observed to be reached in 20 min when 100 g/L calcined magnesite was used to remove initial arsenic -

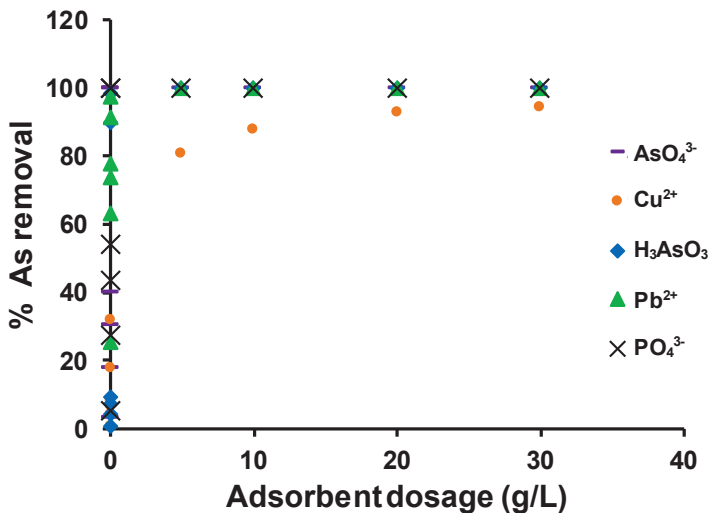


Figure 5. Removal trend from visual MINTEQ for natural water in the presence of 5 g/L magnesite.

concentration of 1 mg/L from water. In the initial concentration of 5.266 mg/L, the percentage removal of 93% in 5 min and 99% in 5 - 8 min was shown at dosage of 5 g/L calcined magnesite. Furthermore, in initial arsenic concentrations between 0.1 and 10 mg/L shaken 3 hours with 5 g/L calcined magnesite, there was observed to be a constant percentage removal of about 99 %, while at the same time, removal capacity (qt) was increasing, ranging between 0.02, and 2.1 mg/g respectively. In initial arsenic concentrations ranging between 1 and 20 mg/L, shaken in 30 min, with 0.5 g/L calcined magnesite, there was a decrease in percentage removal as initial As concentration increased, while the adsorption capacity increased between 1.3 and 10.86 mg/g. For initial As concentrations of 5.266, 10, 20, and 30 mg/L shaken with 50 g/L in 5 hours, there was approximately 100 % removal efficiency, and the adsorption capacity increased from 0.03 to 0.6 mg/g, which indicates that the larger the amount of adsorbent material, the lower the removal capacity.

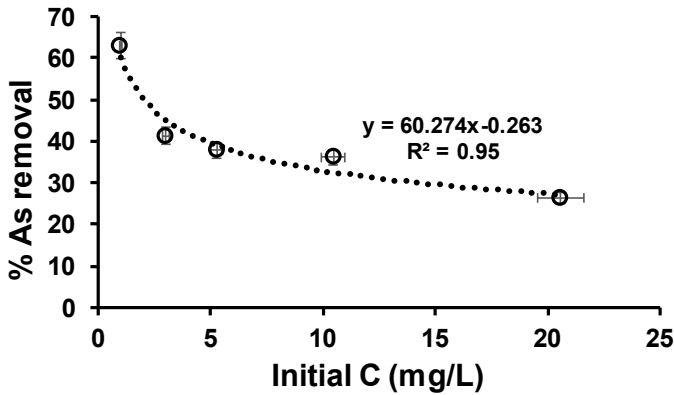


Figure 6. The removal decreases with an increase of initial As when 0.5 g/L is applied for 30 min (Irunde et al., 2023).

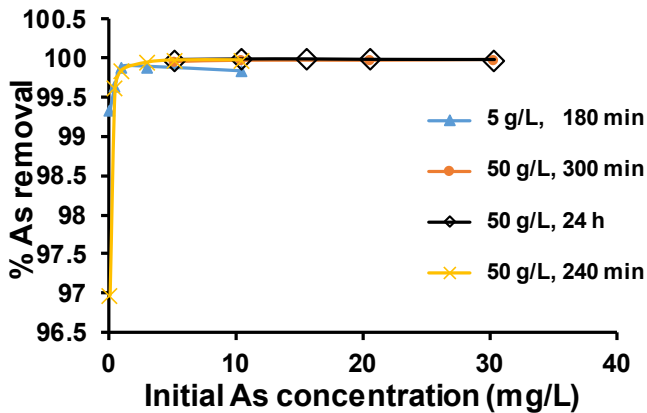


Figure 7. As removal increases with initial As concentration at higher dosage and sufficient contact time.

5.3.1.6. Contact time

An As concentration of 5.266 mg/L shaken with 0.5 g/L calcined magnesite, in 3 hours, was observed to decrease down to 1.1 mg/L. In the same dosage of 0.5 g/L and concentration of 5.266 mg/L, the removal was increasing with time from 20% to 80%. The adsorption capacity also increased with contact time between 2.1 and 8.4 mg/g (Fig. 8).

The As concentration of 5.266 mg/L decreased in 20 minutes to 0.006 mg/L when shaken with 5 g/L calcined magnesite. The percentage removal increased with time from 69 to 100%, and the adsorption capacity increased from 0.7 mg/g in 2 minutes to 1.05 mg/g at 8 minutes, then remained constant for 240 minutes.

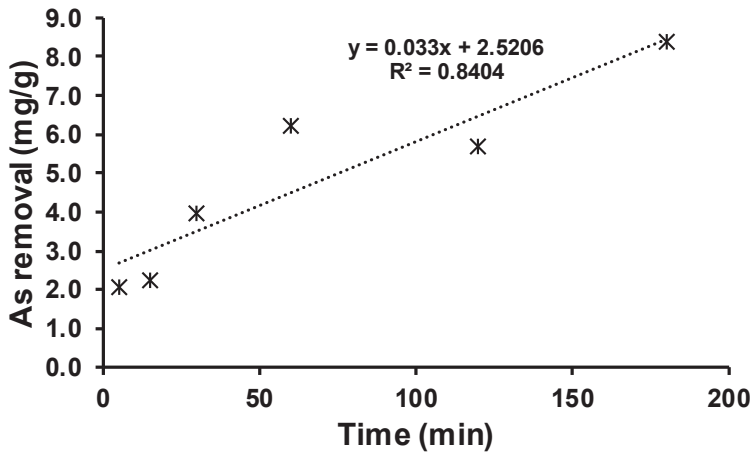


Figure 8. As removal capacity on 0.5 g/L calcined magnesite increases with contact time.

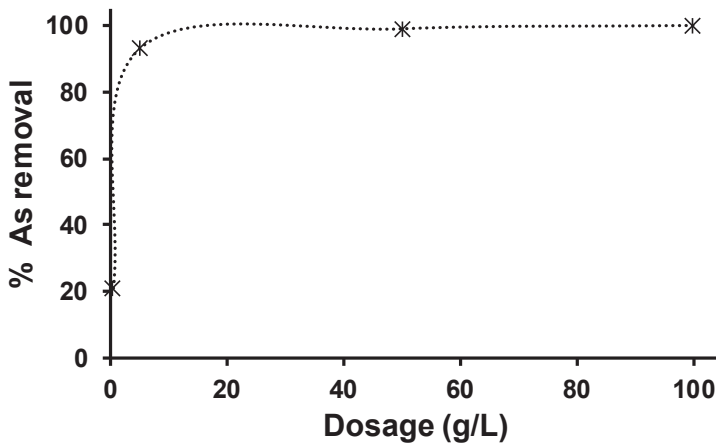


Figure 9. As removal with increase in adsorbent dosage at 5 minutes.

Another observation was that As decreased with time when 5.266 mg/L was shaken with 50 g/L calcined magnesite. The level decreased to 0.0075 mg/L in 30 minutes and reached 0.0039 mg/L in 5 hours. The percentage removal was approximately 100%, and adsorption capacity of 0.105 mg/g in this scenario was constant with time.

5.3.1.7. Dosage

Arsenic removal was observed to increase with an increase in adsorbent dosage (Fig. 9). For the 50 g/L calcined magnesite applied to remove 10.45 mg/L, shaken in 5 hours, revealed 100% As removal, and adsorption capacity of 0.2 mg/g. For 5 g/L calcined magnesite, applied to removal 10.45 mg/L, shaken 3 hours revealed 100% removal and adsorption capacity of 2 mg/g. For the 0.5 g/L, shaken with 10.45 mg/L As for 30 minutes, it revealed 36% removal and the adsorption capacity of 7.5 mg/g.

5.3.1.8. pH

The alkaline condition favored As removal since there was a rapid increase in pH once calcined magnesite was mixed with water. It was observed that higher dosage gave a stable pH, and As removal increased from pH 6.8 to 11 (Fig. 10). Thus, at 5 minutes, 0.5 g/L calcined magnesite raised the pH to 8, and removal was 20%, while 5 g/L raised the pH to 10, and removal was 93%. Despite the higher pH of the water, no metals were released in water above WHO limits (Irunde *et al.*, 2023).

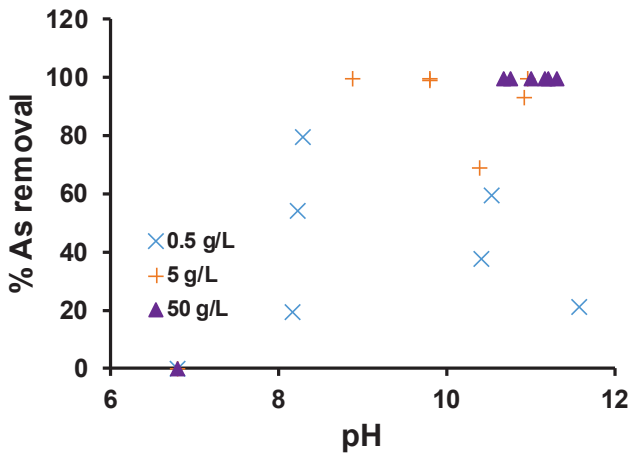


Figure 10. Increasing removal of As with an increase in pH.

5.3.1.9. Chemical reactions for As removal on calcined magnesite

The As concentration was observed to decrease over time, which indicates the chemical reaction was progressing. The final As concentrations remaining in the solution were fitted in kinetic rate laws, and the applied 0.05 g/L, 0.5 g/L, and 5 g/L, fitted first-order kinetic rate law with rate constant k of 0.0003, 0.0079, and 0.3171 min^{-1} . The observations revealed As uptake in the shortest time when a large dosage is applied for water treatment, so the equilibrium time was shortened. The decrease in dosage to 0.5 g/L extended the equilibrium time, which was hypothesized to occur at 30 minutes.

For the prediction of removal limiting factors in the mixture of As solution and calcined magnesite, the results were fitted to simplified kinetic equations, such as pseudo-second-order, intraparticle diffusion, and isotherm model. The As uptake data fitted on intraparticle diffusion was better -

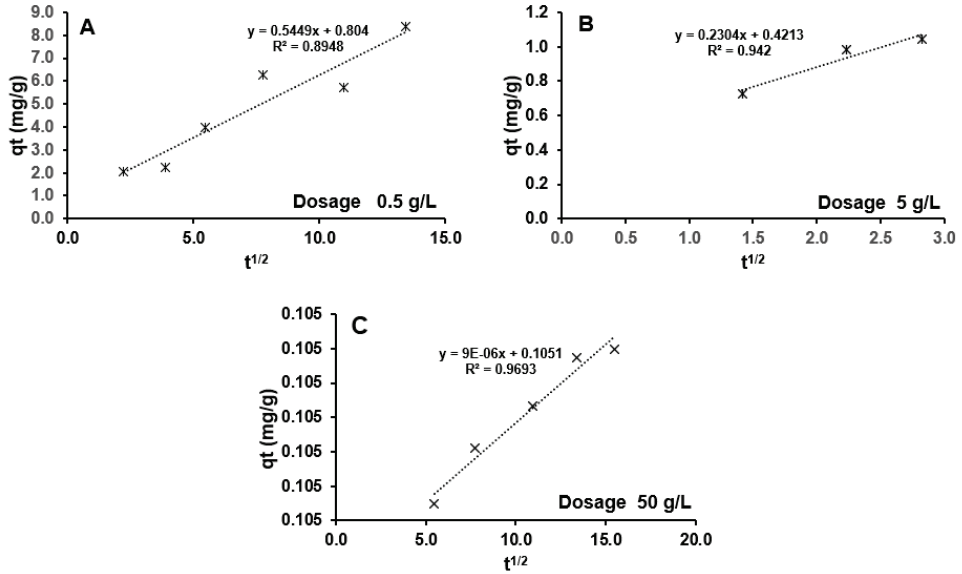


Figure 11. Intraparticle diffusion fitted well 0.5 g/L with K_{id} 0.54 mg/g min^{1/2}.

distributed at the dosage of 0.5 g/L with the rate constant K_{id} 0.54 mg/g min^{1/2} (Fig. 11A). At 5 g/L, the intraparticle diffusion was exhibited in the first 8 minutes of reaction with the rate constant K_{id} 0.23 mg/g min^{1/2} (Fig. 11B). For the dosage of 50 g/L, the rate constant for the intraparticle diffusion K_{id} was 9×10^{-6} mg/g min^{1/2} (Fig. 11C). The best-fit straight line of the intraparticle diffusion did not pass through the origin, indicating the existence of initial boundary layer resistance (Bulut and Tez, 2007).

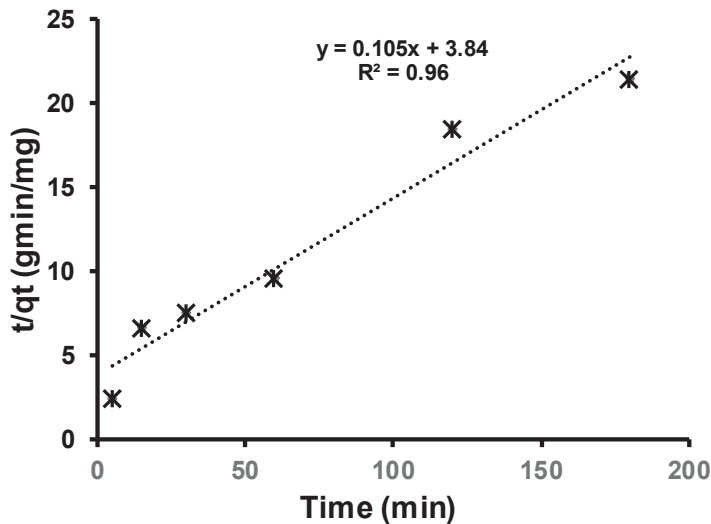


Figure 12. Pseudo second order fit of 0.5 g/L (Irunde et al., 2023).

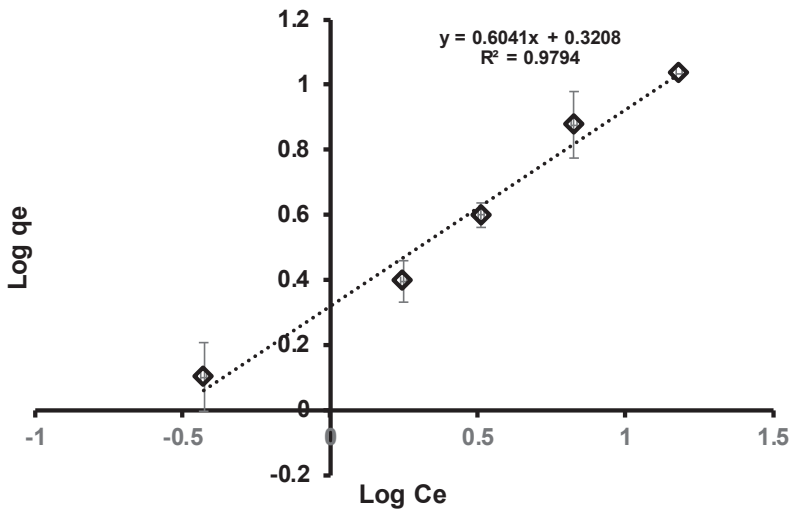


Figure 13. As removal on 0.5 g/L magnesite obeying Freundlich isotherm.

The correlation coefficient R^2 of pseudo-second-order was observed to decrease (1, 0.99, and 0.96) as the dosage decreased from 50 g/L, 5 g/L to 0.5 g/L (Irunde *et al.*, 2023). The best-fit of the As removal explained in pseudo-second-order might indicate that the chemical reaction is a limiting factor. The As uptake data at 0.5 g/L, fitted on pseudo-second-order, exhibited the correlation coefficient R^2 of 0.96 and equilibrium constant rate k_2 of 0.003 g min/mg (Fig. 12).

The Freundlich isotherm model represents the presence of heterogenous surface distributed with multi-site for accommodating contaminants (Chiban *et al.*, 2011). However, the heterogeneity of the surface needs to be confirmed. In the present study, the Freundlich isotherm linear equation was fitted with data from 0.5 g/L shaken with initial As between 1 and 20 mg/L and exhibited a correlation coefficient R^2 of 0.98, distribution coefficient k_f of 0.87 mg/g as well as removal intensity n of 1.54 (Fig. 13).

The Gibbs free energy calculation indicated that the As removal using calcined magnesite was non-spontaneous. The D-R isotherm model confirmed that the removal was controlled by chemical reaction.

5.3.1.10. Arsenic extraction from spent material

Sodium hydroxide (0.1 M NaOH) was mixed with 1 g wet calcined magnesite that was spent on 10 mg/L As removal at pH 11.89 and agitated for 2 hours. The As recovery was only 8%, which means the leaching solution was not perfect for the purpose. Other elements leached during As extraction process were Ca, Fe, and Mg, which were below WHO guidelines.

5.3.1.11. Statistics of linear regression and neural network

The dependent and independent variables, such as concentration, contact time, dosage, and pH, yielded useful information when simulated in SPSS version 28 for linear regression and artificial neural networks (Irunde *et al.*, 2023). Linear regression (Table 3) indicated that all models in terms of dosage (0.05 g/L, 0.5 g/L, 5 g/L, and 50 g/L) applied for arsenic removal were significant at probability value (p -value) 0.002, 0.007, 0.013, and <0.001 , respectively.

The reduction of As concentration was strongly positively correlated ($r \geq 0.9$) to contact time and pH. The most significant parameter that might influence As removal from water was pH especially

Table 3. Linear regression analysis for magnesite.

Dosage g/L	Model <i>p</i> -value	F	R ²	r	Adj. R ²	Std error	Parameter, <i>p</i> -value
0.05	0.002	38.31	0.95	0.975	0.93	0.08	pH, 0.001
0.5	0.007	21.56	0.915	0.957	0.87	0.5	Time, 0.003
5	0.013	26.2	0.946	0.97	0.91	0.6	Time, 0.019 pH, 0.014
50	<0.001	294.8	0.995	0.997	0.99	0.2	pH, <0.001

observed when 50 g/L was applied. Linear regression simulation of the dosage 0.05 g/L exhibited a small error of 0.08, indicating a suitable dosage for water treatment, but it is preferable for the treatment of As concentration below 5 mg/L. The best dosage for the removal of high As concentration above 5 mg/L was predicted as 50 g/L with standard error of 0.2 (Table 3).

The artificial neural network simplified to predict that pH was 100% normalized importance factor that influenced As removal when calcined magnesite was applied while the normalized importance of the contact time was 80%.

5.3.2 Bauxite (Paper IV)

5.3.2.1. Bauxite characterization

The red bauxite collected from Kwemashai, Lushoto, Tanzania, was analyzed in X-ray diffraction (XRD) under X-pert High-Score-Plus and showed the presence of phases such as gibbsite, iron oxide, aluminium oxide hydrate, and aluminium silicate compounds (Fig. 14A, paper IV). The calcined bauxite, the presence of hematite, and aluminium oxides was observed. In the spent material, there were traces of arsenic phases (silver arsenide), in the calcined bauxite but not the raw bauxite.

The XRD spectrum was complicated by the presence of iron oxide (Fe₂O₃) in the bauxite sample. The XRD patterns (Fig. 14) also reveal a shift or disappearance of the iron oxide peak from raw bauxite to calcined and spent bauxite. Although the As phase was not detected in the raw bauxite sample, the acid-digested bauxite samples revealed 65.34 mg/L Fe, which causes noise in the XRD spectrum background, and 0.0058 mg/L trace arsenic was observed (Paper IV).

In the field emission scanning electron microscope, there was a higher oxygen content percentage by weight. The elemental content for oxygen (O₂), aluminium (Al), and iron (Fe) were 68.84%, 18.41%, and 4.74%, respectively, which indicates high levels of aluminium oxides and iron oxides (Paper IV).

The Benuer Emmet Teller (BET) analysis of bauxite sample revealed reduction in surface area after calcination, from which the raw bauxite exhibited surface area of 263.06 m²/g and dropped to 151 m²/g after furnace heating at 500 °C (Paper IV). The bauxite sample can be termed a heterogenous material as was revealed in SEM, due to the composition of many elements in the material (Mohapatra *et al.*, 2008).

5.3.2.2. Batch experiment

5.3.2.3. Natural water with bauxite treatment

The natural water sample that was analyzed revealed the presence of cations and anions, of which arsenate 0.117 mg/L, fluoride 2.3 mg/L, and sulphate 479.8 mg/L exceeded the recommended guideline for drinking water of 0.01 mg/L, 1.5 mg/L, and 250 mg/L respectively (Cotruvo, 2017). Thus, removal was important for the safety of drinking water consumers.

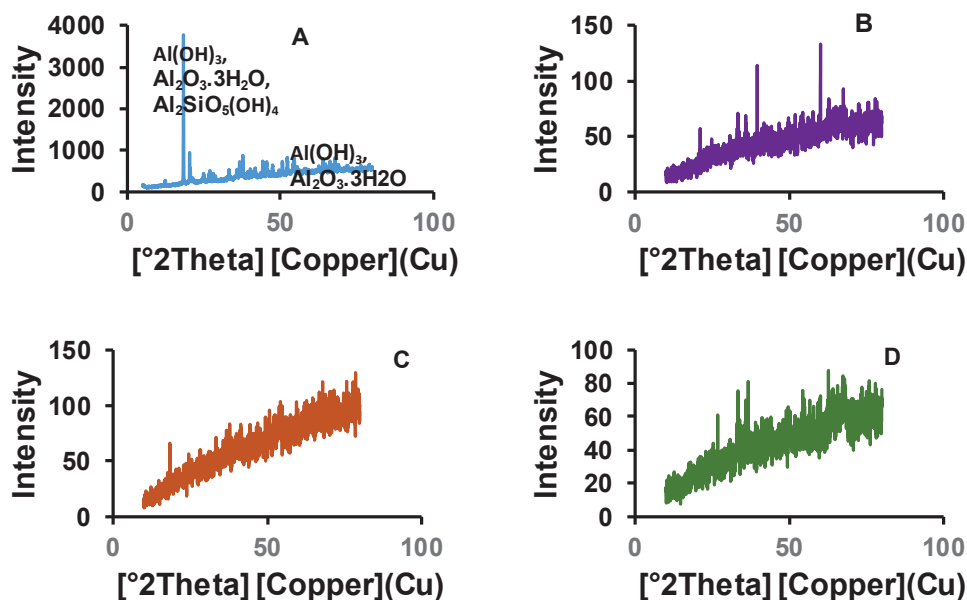


Figure 14. XRD spectrum of A) raw bauxite, B) calcined bauxite, C) raw spent bauxite after As removal, D) calcined spent bauxite after As removal (Paper IV).

The As and fluoride removal was seen in the Visual MINTEQ model (under selection of gibbsite database, which was the dominant phase in bauxite sample) to increase with an increase in dosage; however, the pH significantly affected the process. There was higher As and fluoride removal at lower pH 4, fast equilibrium, and the removal declined as pH increased despite the higher dosage (Paper IV), similar to the reported Lewis adsorption mechanism (Cumbal and Sengupta, 2005). The lower the pH, the higher the As removal, and less dosage added (Paper IV). In Figure 15, the removal of As, and fluoride at pH 7.5 reached saturation point at below 50 g/L gibbsite (Paper IV). There was a similar path for As, and fluoride removal at pH 6.5, and despite the removal decreased as pH increased, the fluoride removal was slightly higher than As when pH increased from 7 to 11 (Paper IV). Lead and cadmium were highly removed at pH 7.5, while manganese removal was very low (Fig. 15, from Paper IV).

Species of As was affected by pH as singly charged As ($\text{H}_2\text{AsO}_3^{-1}$) had higher concentration at pH between 4 and 5 (Paper IV). The doubly charged As ($\text{H}_2\text{AsO}_5^{-2}$) dominates between pH 7.5 and 10 with higher concentration (Paper IV). The saturation phases in the solution appeared from pH 5 as PbMo_4 with saturation index of 0.9 (Paper IV). For the pH 7.5, chloropyromorphite and hydroxyapatite precipitate at the saturation index of 4.9 and 4.7, respectively (Paper IV). The saturation index of the hydroxyapatite was observed to increase with pH and reached 13.2 at pH 10, from which it enhances fluoride removal increase than As (Paper IV).

In the natural water, the application of 100 g/L calcined bauxite removed 0.0053 mg/L and 0.117 mg/L As(V), which exhibited high removal between 98% and 99% (Paper IV).

5.3.2.4. Arsenic solution prepared in the laboratory

5.3.2.5. Dosage

Arsenic percentage removal at 30 min was observed to increase with dosage (Fig. 16, from Paper IV). The removal increased rapidly from dosage 0.5 g/L, with the removal of 19%, and reached equilibrium at the application of 5 g/L with 99% (Fig. 16).

Limitation of dosages was observed as 5 g/L could lower As levels ranging between 0.1 and 3 mg/L to below 0.001 mg/L As within 3 hours, while 5.3 mg/L As was lowered to below 0.005 mg/L (*Paper IV*). Thus, 5 g/L was sufficient to remove As to below the WHO-recommended guideline for drinking water of 0.01 mg/L (WHO, 2017; Cotruvo, 2017). The dosage of 50 g/L was sufficient to lower higher As concentrations ranging between 10 and 30 mg/L to 0.003 mg/L, which is below 0.01 mg/L of WHO guideline (*Paper IV*). The dosage of 0.5 g/L was recommended for lower As concentrations below 0.1 mg/L. The alkaline composite was not sufficient to remove As due to high alkalinity, which leached 435 mg/L aluminium (Al) into the water and only lowered 2 mg/L to 0.6 mg/L at 4 hours (*Paper IV*).

In 60 min, observations show 1 mg/L As was decreased to 0.003 mg/L when 100 g/L of raw and calcined bauxite were applied (*Paper IV*).

For the adsorption capacity, the results showed that the adsorption capacity was increased with a decrease in dosage; thus, the lower the dosage, the higher the adsorption capacity (*Paper IV*). The adsorption capacity of 0.89, 0.21, and 0.0095 mg/g were exhibited by 0.5 g/L, 5 g/L, and 100 g/L, respectively, with the agreement to the 0.09-1.37 mg/g reported by Bhakat *et al.* (2006).

5.3.2.6. The impact of initial As concentration

The percentage removal decreased with an increase in initial As concentration between 0.1 mg/L and 30 mg/L, as presented in Figure 17A (from *Paper IV*). For the higher dosages of 50 g/L and 5 g/L, the removal occurred rapidly up to 99% and remained constant throughout the process (*Paper IV*). The removal percentage decreased rapidly as initial As concentration increased when the low dosage of 0.5 g/L calcined bauxite was applied and shaken for 30 min (Fig. 17A, *Paper IV*).

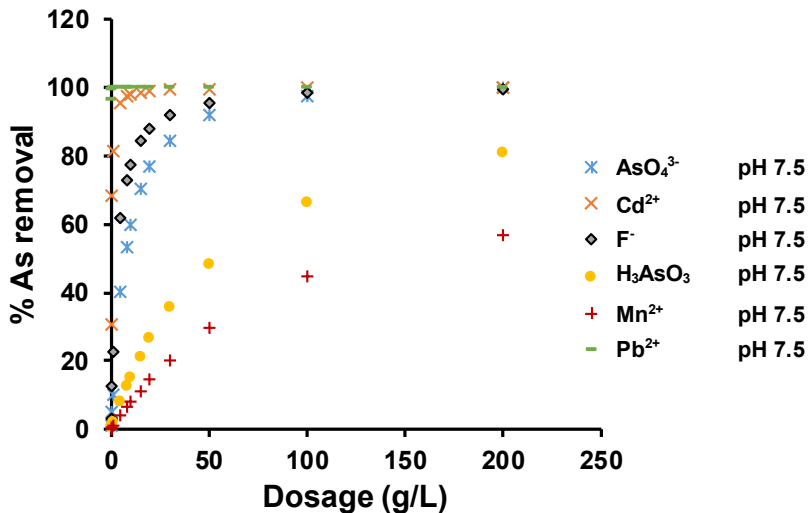


Figure 15. Visual MINTEQ simulation for As and trace elements removal on gibbsite (*Paper IV*).

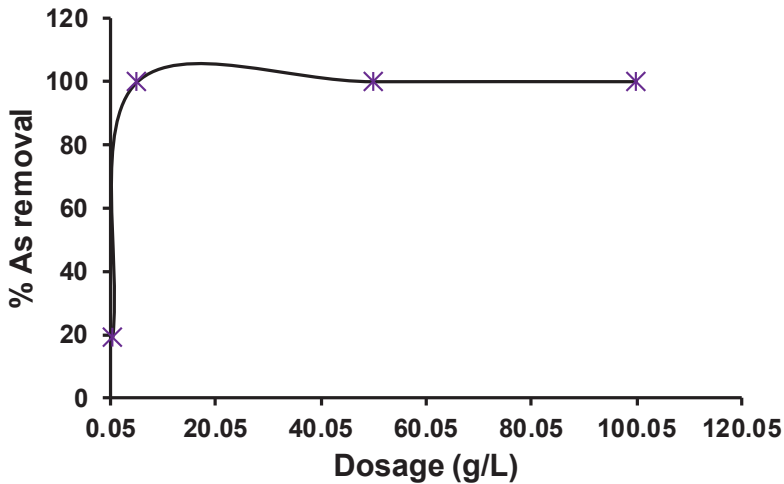


Figure 16. As removal increases with an increase in dosage at 30 min (Paper IV).

The adsorption capacity was found to be increasing with an increase in initial As concentration from 1 mg/L to 20 mg/L (Fig. 17B, from *Paper IV*). The value of adsorption capacity ranged from 0.9 to 6.3 mg/g; this was similar to the results reported by *Bhakat et al. (2006)*, where capacity ranged from 0.999 to 1.37 mg/g from the initial concentration range of 0.5 mg/L to 8 mg/L (*Paper IV*).

5.3.2.7. The impact of pH

The visual MINTEQ simulation indicated that percentage of As removal was higher at lower pH 4 which decreased as pH increases is similar to the phenomena reported by *Mohapatra et al. (2008)*. It was reported that As removal is influenced by pH and controlled through ligand exchange, coulombic attraction, and repulsion from which the point of zero charge (pHpzc) for calcined bauxite was 7.54, and 7.76 for the raw bauxite (*Mohapatra et al., 2008*). The amphoteric nature of the bauxite (Eqn. 26 and 27 below) to shift equilibrium to the right or left, trying to neutralize solution was previously reported (*Mohapatra et al., 2008*). It is observed that at neutral pH 7, the raw bauxite lowered pH from 7 to 6, which correlates to the hypothesis that bauxite acidity regulates pH of the water (Table 4).



There was marginal increase in pH for acidic solutions (Table 4), which can be explained by the amphoteric nature of the bauxite. The presence of oxides in the calcined bauxite increased pH of the water. From XRD data, iron oxide (Fe_2O_3) was naturally present in the bauxite, even before calcination, and it affected the X-ray analysis of the bauxite by creating background noise in the spectrum. The calcination process increases oxides in the material and, thus, raises the pH to a greater extent. The bauxite is also reported to have an ability to absorb carbon dioxide (CO_2) (*Han et al., 2017; Yadav et al., 2010*) to form metal carbonates, which can dissociate to form carbonate ions that raise pH. The ability of bauxite to act as a carbon sink was revealed when bauxite calcined in the presence of magnesite raised pH. The bauxite calcined in the furnace, in the presence of magnesite, gave a rise in pH, while the bauxite calcined (newly calcined) in the absence of magnesite lowered the pH.

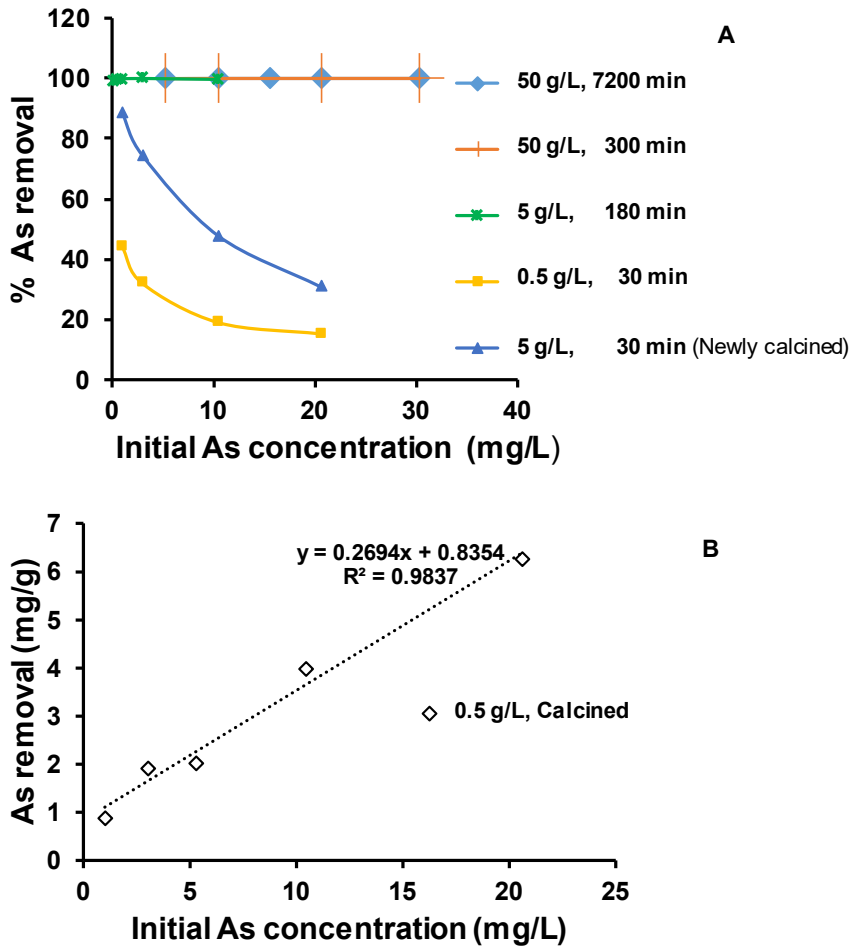


Figure 17. Effect on initial initial As removal: A) %As removal, B) Removal capacity (mg/g) (Paper IV).

Table 4 The measured pH of bauxite.

	Bauxite (g)	Volume (mL)	Initial pH	Final pH
Raw	2	10	4.2	5.68
	2	10	2.31	3.42
	10	100	1.73	2.3
	10	100	2.46	4.4
	10	100	7.0	6.07
Calcined	2	10	2.26	5.69
	2	10	1.51	3.97
	10	100	7.0	7.4

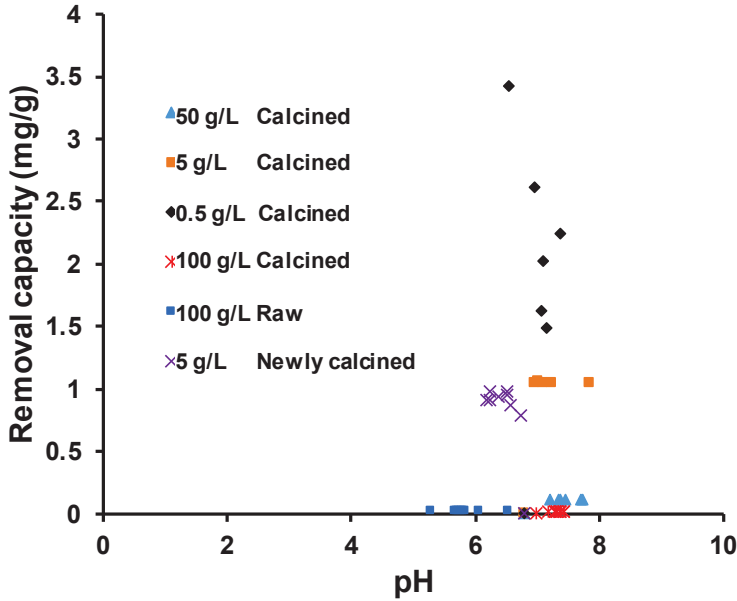


Figure 18. The influence of pH 5 - 7.8 for As removal capacity.

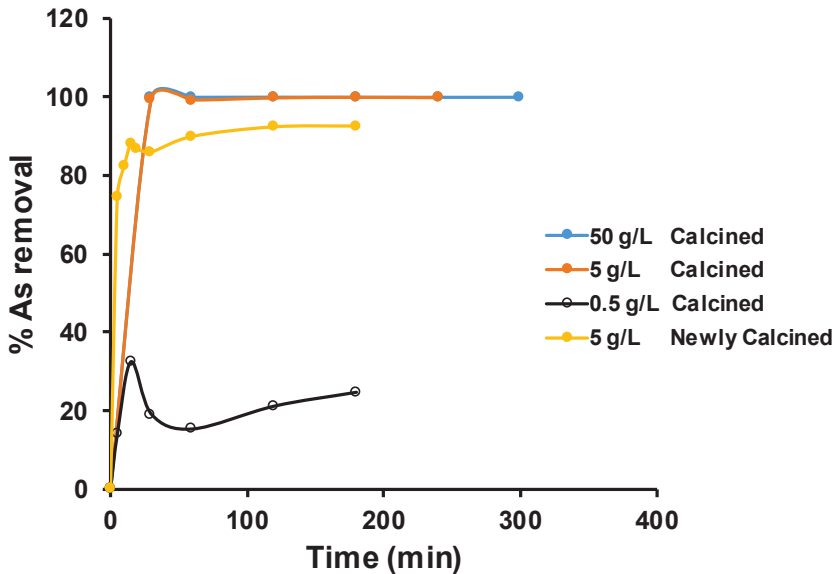


Figure 19. As removal by calcined bauxite with increase in contact time.

The mechanism of As removal is explained through non-specific adsorption (Mohapatra *et al.*, 2008) since the saturation indexes from the visual MINTEQ did not show the formation of Al and Fe precipitation with As at pH range 4 to 10. However, XRD showed the formation of arsenate

with Al and Fe. Therefore, it is suggested that both mechanisms of precipitation and adsorption may occur simultaneously during As removal by bauxite. However, further elucidation with advanced techniques such as extended X-ray absorption fine structure (EXAFS) and with X-ray absorption near edge spectroscopy (XANES) would be valuable to show how As is attached on the adsorbent edge.

In the present study of bauxite application, it was observed that more As removal capacity occurred between pH 5 and 7.8, and lower dosage of 0.5 g/L gave a higher removal capacity (Fig. 18). It was previously reported that the maximum As removal was within pH 4 to 7 (Mohapatra *et al.*, 2008), and pH range 2 to 8 (Bhakat *et al.*, 2006) and the removal decreases as pH increases above 8.

5.3.2.8. Contact time influence

The longer contact time caused an increase in As percentage removal (Fig. 19). There was a rapid percentage removal increase in the first 5 to 30 minutes before it reached equilibrium. The maximum As removal to below 0.01 mg/L recommended by WHO was achieved from the application of 50 g/L and the equilibrium was reached before 5 min. The 5 g/L required longer contact time for about 3 hours to lower As below 0.01 mg/L. Improvement of As removal was observed for longer contact time was provided for lower dosages of 0.5 g/L (*Paper IV*).

5.3.2.9. Kinetic reactions

The reduction of As concentration in the solution decreased with an increase in contact time (Fig. 20). The equilibrium time for higher dosage was approximately reached before approximately 5 minutes (Fig. 20).

The hypothesized CO₂ sink with calcined bauxite in the presence of magnesite exhibited an efficiency reduction for 5.266 mg/L As to below 0.01 mg/L, but this occurred only at higher dosage since lower dosage of 0.5 g/L was not suitable for high As concentrations (*Paper IV*).

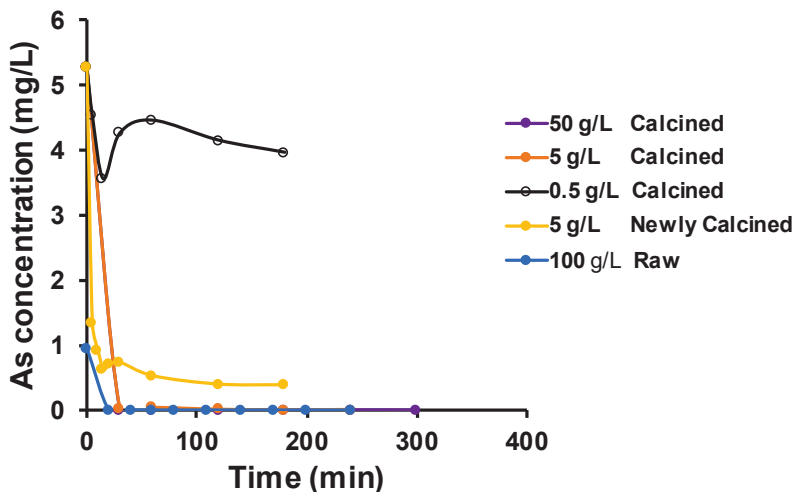


Figure 20. As reduction by calcined bauxite with increasing contact time.

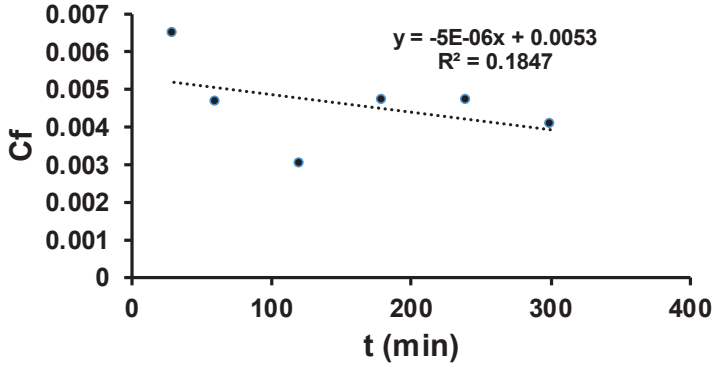


Figure 21. As removal with 50 g/L calcined bauxite is explained by zero order.

The rate law orders were applied to provide an insight into how fast the reaction was during As removal (*Paper IV*). The correlation was poor ($R^2 = 0.18$) for the 50 g/L dosage, which lowered As to below 0.01 mg/L, but the indication is that the zero-order reaction kinetics had a rate constant k of 5×10^{-6} M/min (*Fig. 21*).

Rate constants “ k ” of 0.00001 and 0.0008 M/min from the zero-order rate law were exhibited from the application of the calcined bauxite of 100 g/L and 0.5 g/L, respectively (*Paper IV*). Moreover, the rate constants “ k ” of 0.0003, 0.0093, and 2.2 /M min from the second-order rate law was exhibited from the application of 50 g/L alkaline composite, 5 g/L newly calcined, and 100 g/L raw bauxite, respectively (*Paper IV*). For the rate constant k of 0.0071 /min from the first-order rate law of 5 g/L calcined bauxite application (*Paper IV*).

The kinetics of the reaction for As removal by raw and calcined bauxite fitted well to pseudo-second-order reaction kinetics with $R^2 = 0.99$, which signifies chemical reaction involvement in the process (*Bulut and Tez, 2007*).

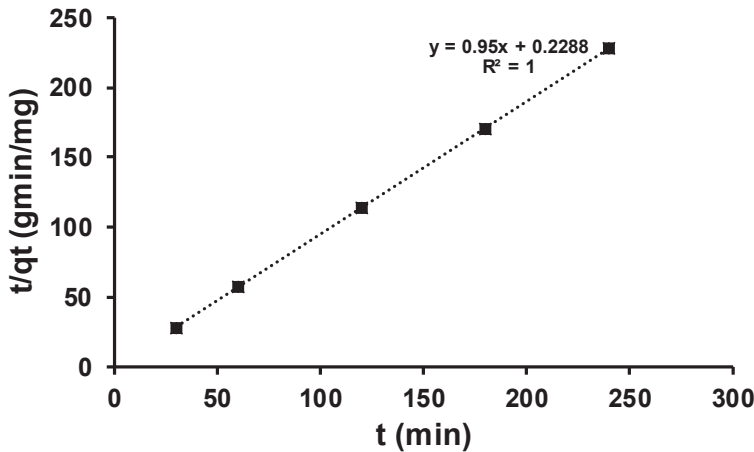


Figure 22. Pseudo second order reaction kinetics for As removal on 5 g/L calcined bauxite (*Paper IV*).

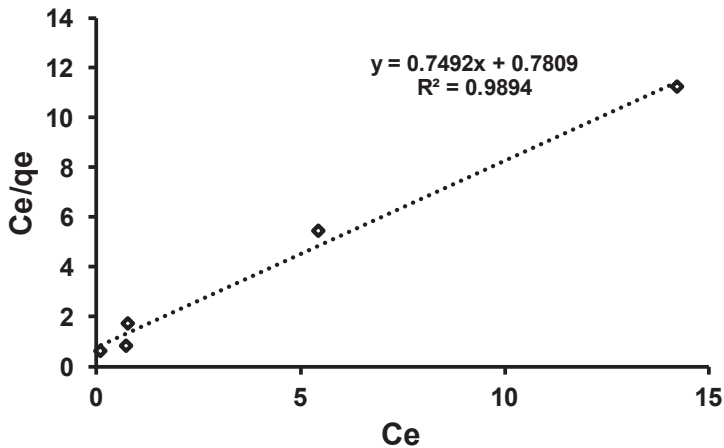


Figure 23. Langmuir isotherm for As removal on 5 g/L calcined bauxite (Paper IV).

The rate constants k_2 for the pseudo-second order were 0.65, 3.9, 17.8, 953, 1198, and 2427 g min/mg from the application of 5 g/L newly calcined, 5 g/L calcined, 50 g/L alkaline composite, 0.5 g/L calcined, 100 g/L raw, and 50 g/L calcined respectively (*Paper IV*). The adsorption capacity q_e of 1.053 mg/g in Figure 22 was correlated to the experimental calculations (*Paper IV*).

The chemical reactions were fitted to a Langmuir isotherm with correlation coefficient R^2 ranging between 0.73 and 1 (*Paper IV*). It was reported previously that the 5 g/L bauxite fitted Langmuir isotherm with maximum adsorption capacity q_m of 1.566 mg/g (Bhakat *et al.*, 2006) and 1.78 mg/g (Mohapatra *et al.*, 2008). The Langmuir isotherm explains better adsorbents with monolayer coverage.

The present study revealed the Langmuir model's maximum removal capacity of 1.33 mg/g (Fig. 23, from *Paper IV*). The Langmuir adsorption was favorable since the calculated R_L was 0.65, which is greater than zero and less than 1.

5.3.2.10. Parameter influencing As removal

Table 5 below represents how linear regression can analyze experimental data to define if there is significant relation between independent and dependent variables relating to the probability value (p -value) of 0.05. For significant models, the parameter with lower p -value was also trained in the neural network as an important parameter for As removal.

For the higher As concentration of 5.3 mg/L, results were non-significant according to probability value of 0.05 (Table 5). The parameters such as pH and contact time were also not significant, which means no relation between predictors As concentration increased. In the low As concentration of 1 mg/L, the model was significant, and the predictors, such as pH and contact time, were significant, which signifies bauxite was suitable for lower As concentrations.

5.3.2.11. Leaching of the spent bauxite material

For the 1 g of bauxite, which was able to lower 10 mg/L to 0.0018 mg/L after 4 hours was mixed with alkaline solution 0.1 M NaOH, and 45.8% As was released into the solution of pH 12.89. It was observed that more aluminium ion about 646 mg/L, was released into the solution at pH of 12.89, which decreased the amount of aluminium in the adsorbent material. The release of aluminium ions into the solution after washing with NaOH was previously reported to lower the ability of the adsorbent (Bhakat *et al.*, 2006; Mohapatra *et al.*, 2008).

Table 5. Parameters influencing As removal from bauxite.

Dosage (g/L)	Model <i>p</i> -value	R ²	R ² adjusted	r	std error	Low <i>p</i> -value	Neural Network
0.5 Calcined	0.441	0.34	0.004		0.5	Time = 0.277	pH
5 Newly calcined	0.082	0.57	0.4	0.75	1.2	pH = 0.06	pH
5 Calcined	0.415	0.44	0.07	0.67	2.1	Time = 0.303	Time
50 calcined	0.126	0.65	0.47	0.8	1.45	pH = 0.11	pH
Combined above	0.035	0.29	0.2	0.5	1.9	Time = 0.021	Time
100 Calcined	0.014	0.71	0.62	0.84	0.2	pH = 0.011	pH
100 Raw	0.022	0.67	0.57	0.8	0.2	pH = 0.018	pH

5.3.3. Gypsum. (Paper V)

5.3.3.1. Characterization of gypsum

The X-ray spectrum analyzed in X-pert high score-plus shows phases of calcium sulfate dehydrate and calcium sulfate hydrate in raw gypsum with peaks at 2θ between 11.8° and 54.6° (Paper V). The calcined gypsum at 500°C showed the presence of calcium sulphate and calcium carbonate (Fig. 24, from Paper V)

The phases of calcium oxide (CaO) and calcium peroxide (CaO₂) observed under X-pert high score restriction was positioned at $2\theta = 26.8^\circ$, and 29.6° (CaO), and 29.6° (CaO₂), respectively (Paper V).

In the Field emission SEM-EDS, the analysis showed the elemental composition of calcium (Ca), oxygen (O), carbon (C), and sulfur (S) with percentages by weight around 12%, 62%, 13%, and 10% respectively (Paper V). The surface area of the calcined gypsum decreased by $9\text{ m}^2/\text{g}$ to $26\text{ m}^2/\text{g}$ since the fine powder forms aggregation when kept compacted for a long time (Paper V).

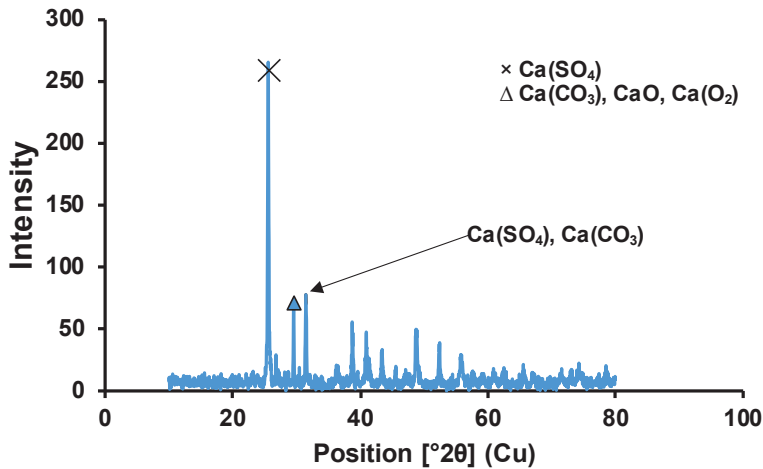


Figure 24. XRD diffraction of calcined gypsum showing main phases (Paper V).

5.3.3.2. The natural water

The composition of cations and anions present in natural water from Masinki stream (Irunde *et al.*, 2023) was simulated in visual MINTEQ to observe the As removal with an increase in dosage, under pH influence. The mineral saturation index with an increase in pH predicts removal efficiency at higher pH than at lower pH (Paper V).

The simulation revealed that As removal was increasing with dosage, but more removal occurred at higher pH between 9 and 10 (Fig. 25, Paper V). For the arsenate and phosphate having similar characteristics, the difference was revealed in visual MINTEQ that phosphate removal was higher than arsenate, at lower pH up to pH 7, while As is favored at pH 9 – 10 (Fig. 25, Paper V).

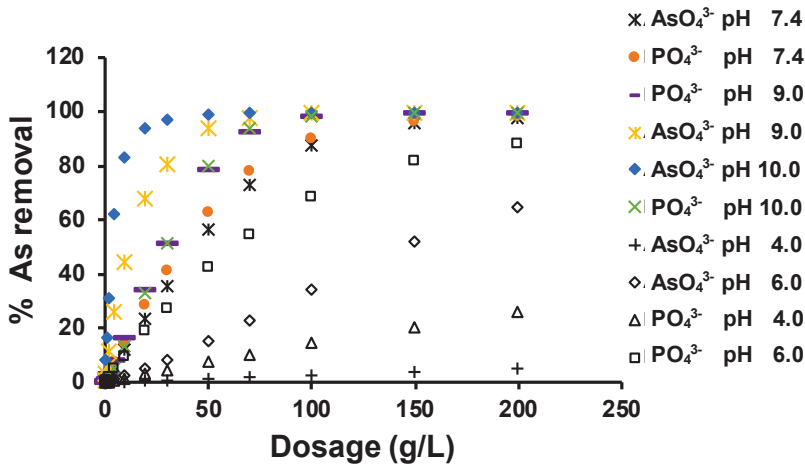


Figure 25. Visual MINTEQ simulation for As removal by calcined gypsum with dosage effect (Paper V).

In pH 6, the As percentage removal was increased with dosage, as 1.3%, 2.6%, 15%, 34%, and 64.9%, from the dosage of 5 g/L, further, 10 g/L, 50 g/L, 100 g/L, and 200 g/L, respectively, while for phosphate removal, 5%, 9.9%, 42.7%, 68.6%, and 88.5%, respectively, with dosages (Fig. 25). The phosphate removal dropped much at pH 9, for lower dosages 0.5 g/L – 50 g/L (Fig. 25).

The application of 100 g/L calcined gypsum on natural water revealed 99 % As(III) removal and 84 % As(V) at pH 9 (Paper V). The batch experiment shows little leaching of dimethyl arsenate (DMA) from the calcined gypsum (Paper V).

5.3.3.3. Arsenic solution prepared in the laboratory

This section summarizes the parameters effecting As percentage removal and removal capacity from the prepared solution as well as reaction kinetics phenomena when gypsum was applied.

5.3.3.4. Initial As concentration effect

Arsenic removal percentage was observed to decrease with higher As initial concentration (Fig. 26). The application of 50 g/L calcined gypsum (Fig. 26), stirred for 4 hours, removed As from initial concentration ranged between 0.1 and 10 mg/L, and the removal decreased from 83% to 54%, respectively.

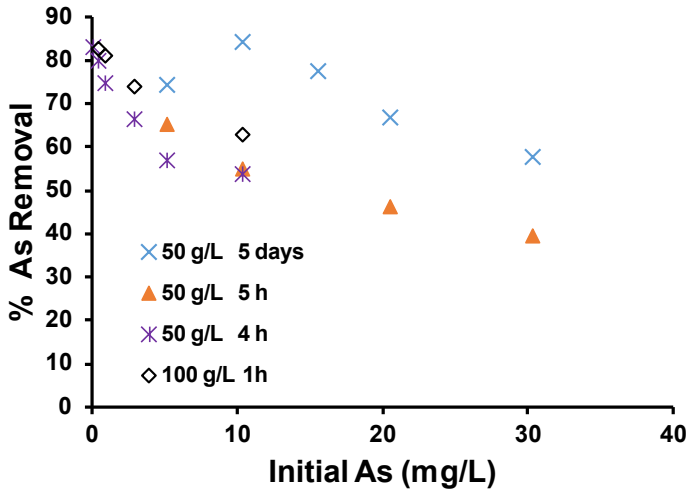


Figure 26. The decrease in As removal by calcined gypsum as the initial As concentration increases (Paper V).

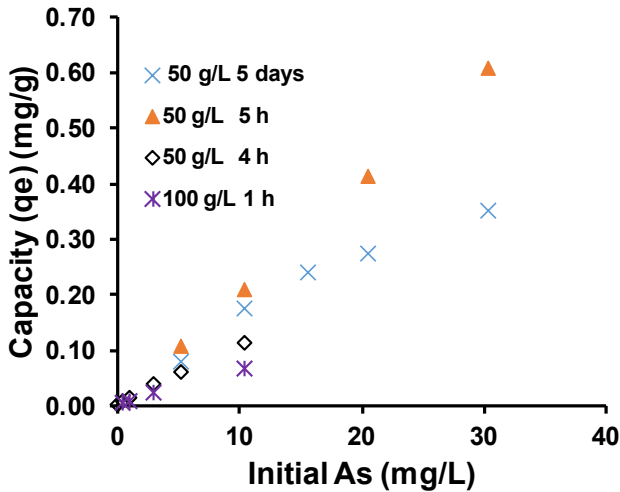


Figure 27. Adsorption capacity on additions of calcinated gypsum increases with increase in initial As concentration (Paper V).

The adsorption capacity was observed to increase with an increase in initial As concentration (Fig. 27, from Paper V). The trend of removal capacity increasing with an increase in initial As concentration, indicates an adsorption mechanism, as was previously reported (So et al., 2008). The removal capacity was also increased with the decrease in adsorbent dosage (Fig. 27, from Paper V), from which the lower dosage exhibited more adsorption capacity, similar to our previous study on As removal using calcined magnesite (Irunde et al., 2023).

5.3.3.5. The effect of contact time

The percentage As removal was observed to increase with extended contact time (Fig. 28, Paper V). Thus, for the 50 g/L calcined gypsum, shaken with 5.3 mg/L for 5 hours exhibited removal as 43%, 47%, 54%, 58%, and 60%, which indicate rapid increase in removal followed by constant removal after 3 hours (Fig. 28). This can predict equilibrium time at 3 hours, than the previously reported 12 hours from gypsum (Chen *et al.*, 2014) and calcite 25 hours (So *et al.*, 2008).

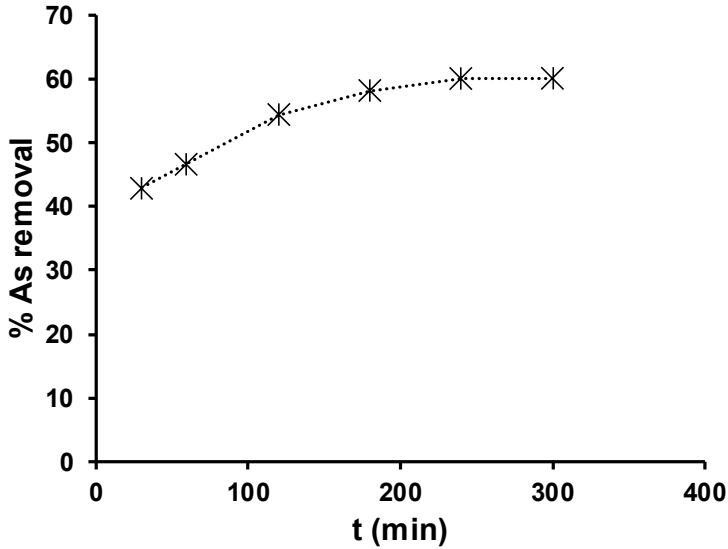


Figure 28. As removal from a solution with 5.3 mg/L As by addition of 50 g/L calcined gypsum, showing the effect of contact time (Paper V).

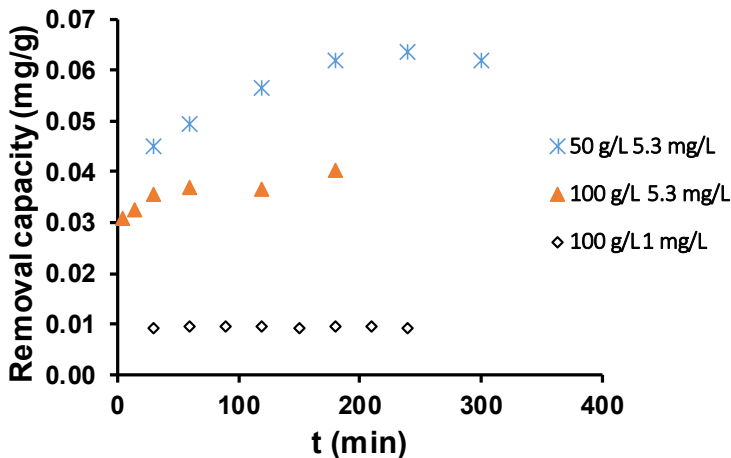


Figure 29. Increasing As removal capacity of calcined gypsum with contact time (Paper V).

Table 6 Removal increased and capacity decreases with calcinated gypsum dosage.

As mg/L	5.3		1
Dosage (g/L)	50	100	100
As removal (%)	59	76	99
Removal capacity (mg/g)	0.06	0.04	0.01

The removal capacity increased rapidly within the first 60 minutes (Fig. 29, from *Paper V*) before reached a constant state. The lower dosage of 50 g/L for the gypsum application exhibited a more rapid increase in adsorption capacity (Fig. 29).

5.3.3.6. Dosage increase

The removal percentage was observed to increase with an increase in dosage (Table 6). For dosage of 50 g/L stirred with initial As of 5.3 mg/L, there was a removal of 56%, which increased to 76% when 100 g/L was added (Table 6). The trend of increase in removal percentage with dosage was reported previously (Chen *et al.*, 2014). The increase in active sites is also influencing removal increase (So *et al.*, 2008). The adsorbent capacity was decreased as dosage increased, which was also previously reported (Chen *et al.*, 2014).

5.3.3.7. pH impact

The observations revealed the neutral pH 6.8 solution as a better working solution during the application of raw gypsum since lower pH 4.2 and 1.5 were raised to 8 and 6, respectively (*Paper V*). The main phases present in the gypsum were calcium sulphate, and calcium carbonate, which formed calcium oxide during heating at 500 °C. The oxides present in the calcined gypsum rise pH to 9 (*Paper V*). There was a variation of pH between 7 and 9 for water samples treated by calcined gypsum in the present study, attributed to the amount of oxides converted from heating. The As removal at around pH 9 was previously reported (Bardelli *et al.*, 2011; Román-Ross *et al.*, 2006; So *et al.*, 2008).

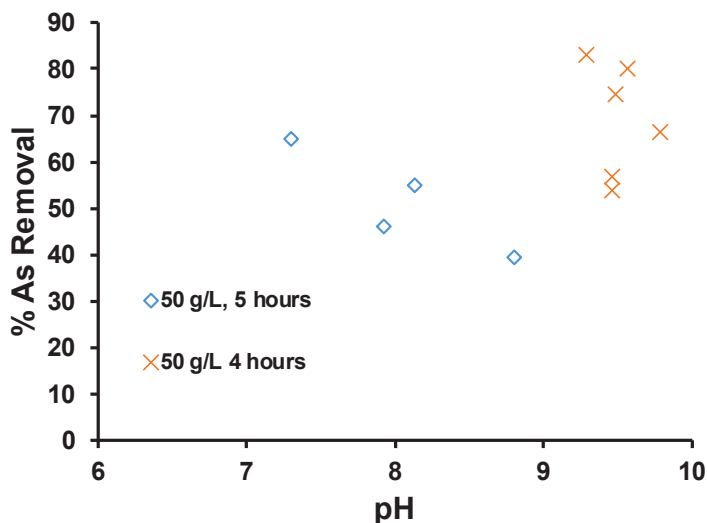


Figure 30. Variation of the As removal percentage by calcinated gypsum with pH.

In Figure 30, the As percentage removal is seen to increase with an increase in pH. It was a challenge to relate pH with percentage removal or adsorption capacity since most of the sample solution had pH of around 7 to 8, and removal was similar to the samples with pH of 9 to 10. This phenomenon of little correlation between the pH effect and As removal was previously reported (So *et al.*, 2008). In the present study, the highest 83% removal occurred around pH 9.3 (Fig. 30).

5.3.3.8. Kinetic reactions

The equilibrium time was observed to be dependent on As initial concentrations (*Paper V*). The high As concentrations above 5 mg/L require longer contact time to reach equilibrium. Figure 31 showed 50 g/L calcined gypsum caused 5.3 mg/L As to attain equilibrium after 3 hours. The higher dosage shortened the equilibrium time, which was reported to be 12 hours (Chen *et al.*, 2014).

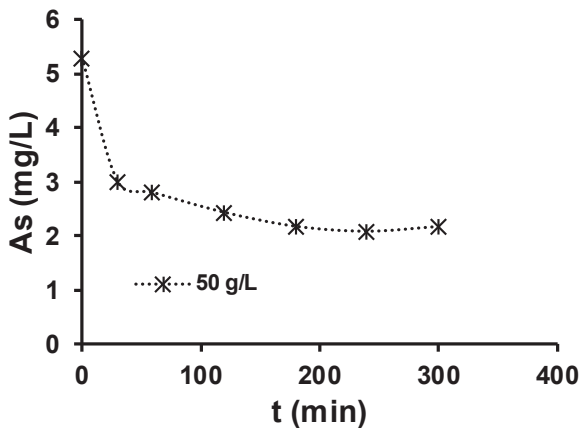


Figure 31. As concentration decreased when 50 g/L calcined gypsum was added to 5.3 mg/L As, showing equilibrium was reached at around 3 hours.

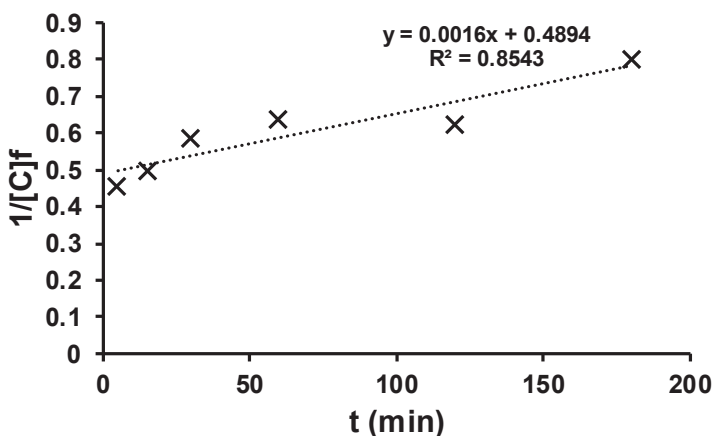


Figure 32. Arsenic removal from application of 100 g/L calcined gypsum obeyed second order.

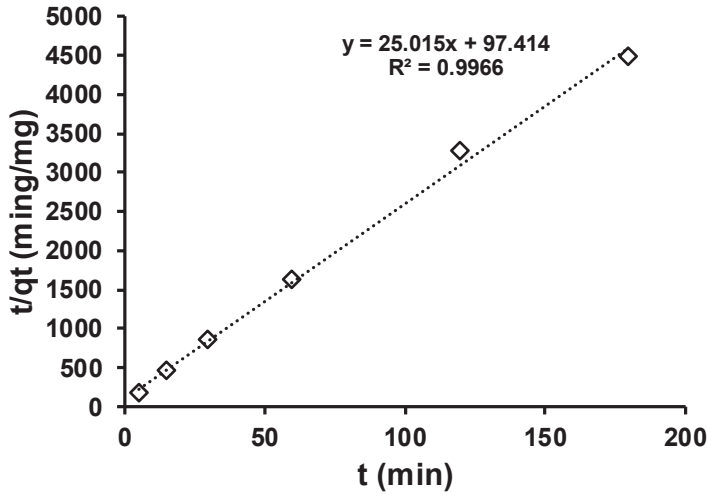


Figure 33. Pseudo second order fitted 5.3 mg/L As removal by 100 g/L calcinated gypsum.

The second-order rate law explained better the reaction between 5.3 mg/L As stirred with 100 g/L (Fig. 32) and 50 g/L with R^2 of 0.85 and 0.91, respectively (Paper V). For the 5.3 mg/L As, the half-life following second-order rate law decreased with an increase in dosage (Paper V). The pseudo-second-order (Bulut and Tez, 2007) fitted 5.3 mg/Las removal with R^2 of 0.99 (Fig. 33, Paper V).

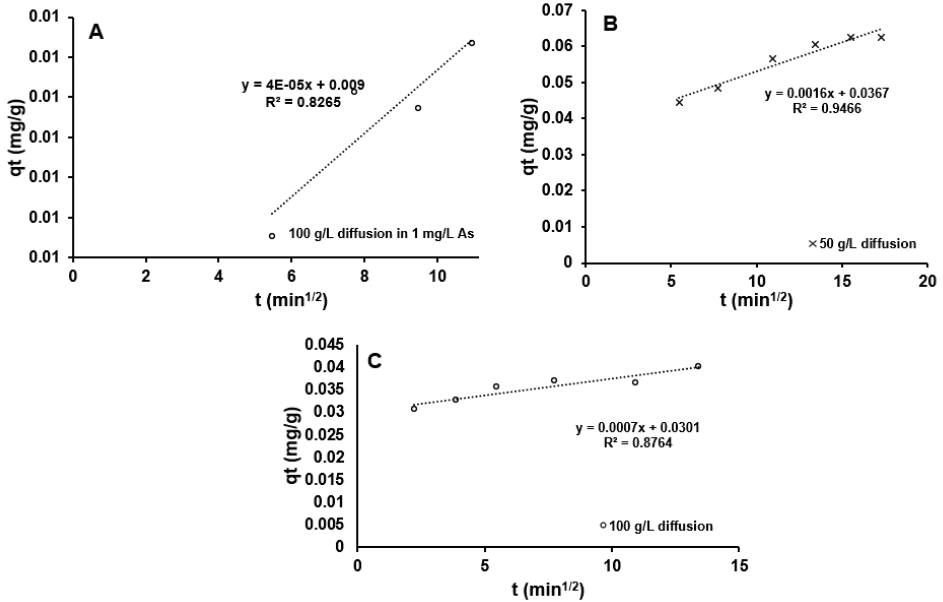


Figure 34. Intraparticle diffusion results for 100 g/L gypsum in 1 mg/L As [A], 50 g/L gypsum 5.3 mg/L [B], and 100 g/L gypsum in 5.3 mg/L As [C].

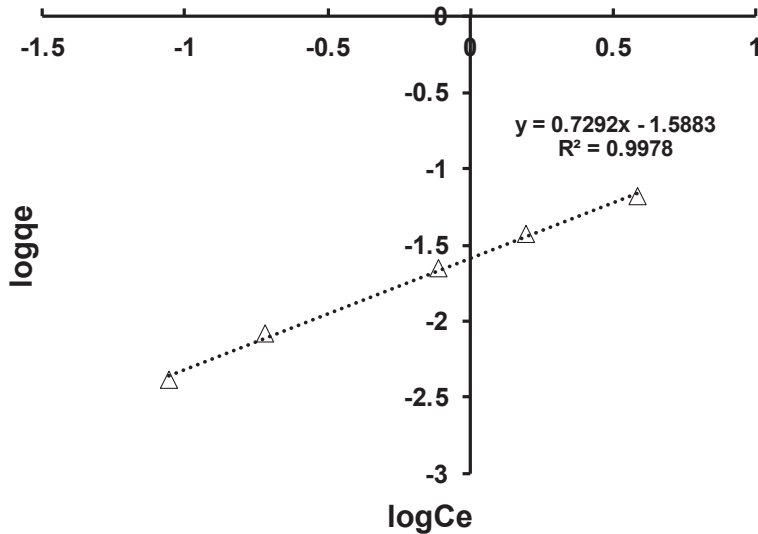


Figure 35. Freundlich isotherm results for 100 g/L dosage of for 5.3 mg/L removal.

The higher the dosage, the faster rate of As removal, while adsorption capacity increases with an increase in initial As concentration. The rate constant (k_2) for pseudo-second-order increased with dosage; 100 g/L exhibited 6.4 g min/mg, which was 5 times more than the application of 50 g/L (**Paper V**). The adsorption capacity (q_e) had a slightly small difference from the application of 100 g/L and 50 g/L.

The removal data fitted intraparticle diffusion with R^2 of 0.83 (Fig. 34A), 0.95 (Fig. 34B), and 0.88 (Fig. 34C) (**Paper V**). The higher dosage of 100 g/L exhibited lower diffusion rate of 4×10^{-5} mg/g min^{1/2} (Fig. 34A) and 0.0007 mg/g min^{1/2} (Fig. 34C). The 50 g/L dosage exhibited higher diffusion rate of 0.0016 mg/g min^{1/2}. The linear fit did not pass through the origin, which is in agreement with the previously reported observations (Bulut and Tez, 2007).

The experimental data obeyed Freundlich isotherm with R^2 of 0.99 (Fig. 35). The convex shape was reported to signify sorption (So *et al.*, 2008), which also indicates the presence of mesoporous structures. The rate k_f was approximately 4 mg/g for both 50 g/L and 100 g/L as well as $1/n$ was observed to be 0.73 (**Paper V**).

5.3.3.9. Leaching of spent gypsum

The spent 50 g/L calcined gypsum was mixed with 10 mL of 0.1 M NaOH and shaken vigorously for 2 hrs at pH 12.47, showed 0.24% As leached in water. Minerals, which were also not leached, were calcium and magnesium (**Paper V**). However, some minerals, such as Al (53.8 mg/L) and Fe (0.0004 mg/L), were released below the WHO recommended guideline (**Paper V**). The leaching solvent was not suitable for As release at the specific pH since gypsum stabilizes As at pH between 10 and 13.

5.3.3.10. Parameters that influence gypsum for As removal

The linear regression of the experimental data simulated on SPSS version 28 showed 100 g/L dosage as the best system, which had less error and was significant at probability value (p -value) of <0.001. The 98% was explained by pH and time (**Paper V**). The pH was a significant parameter at the p -value of <0.001. The results were positively correlated with an adjusted R^2 of 0.97 (**Paper V**). The application of 50 g/L was not significant, with an adjusted R^2 of 0.45 (**Paper V**).

5.4. THE MINI-SCALE COLUMN EXPERIMENT

The mini-scale column experiment (Fig. 36) was conducted to evaluate flow rate and As percentage removal. The major cations, trace elements, metalloids, and anions were analyzed from the column sample collected at 30 min (Table 7) since this was hypothesized from the batch experiment as suitable for equilibrium to occur. The elements calcium (Ca), iron (Fe), magnesium (Mg), potassium (K), silicon (Si), sodium (Na), sulfur (S), aluminium (Al), arsenic (As), barium (Ba), boron (B), cadmium (Cd), chromium (Cr), copper (Cu), lead (Pb), manganese (Mn), mercury (Hg), molybdenum (Mo), nickel (Ni), phosphorus (P), strontium (Sr), and zinc (Zn) were analyzed (Table 7). The As level of 92 g/L exceeded WHO guideline of 10 µg/L. For anions, the concentration of chloride (Cl⁻), fluoride (F⁻), nitrate (NO₃⁻), and sulfate (SO₄²⁻) were 104, 2.47, 37.7, and 82.2 mg/L, respectively (Table 7), and fluoride exceeded the WHO recommended guideline of 1.5 mg/L.



Figure 36. Mini-scale column to evaluate efficiency of magnesite, bauxite, gypsum, and BGM (1:1:2).

The results from outlet sample showed that about 15 to 20 mL (Table 7) were collected from columns within 30 min, and the flow-rate at 30 min ranges between 0.5 and 1 mL/min, which is lower than the previously reported flow rate (Liu *et al.*, 2014; Roy *et al.*, 2013). The adsorption capacity of As on magnesite was 0.138 mg/g, which agrees with findings from the batch experiments (Irunde *et al.*, 2023).

The arsenic outlet concentration dropped from 92.2 µg/L to 0.07 µg/L in magnesite, 0.327 µg/L in bauxite, 1.46 µg/L in gypsum and 0.126 µg/L in BGM (Table 7). Fluoride decreased from 2.47 mg/L to 0.23 mg/L in bauxite, to 0.59 in gypsum, 0.78 in magnesite and 0.94 mg/L in BGM.

The uptake of each element is shown in Figure 37 and Table 7. The removal was above 90% in many cases, and the magnesite uptake of As was above 99%, marginally higher than bauxite and gypsum.

The mini-scale column packed with magnesite (Fig. 37) showed high removal in the order $\geq 59\%$, ranging between 59.4% nitrate and 99.9% of As, Zn, Pb, and Cu. Despite the fact that magnesite had high efficiency to remove broad range of metals and non-metals, it exhibited an increase of magnesium in water for about 60 mg/L, the same as 59% (Table 7).

The As removal capacity for 20 g magnesite in the mini-scale column (Table 8) was 0.14 µg/g from the flow rate of 1 mL/min. The Thomas kinetic rate constant K_{TH} from the magnesite column for As removal at 30 min was evaluated as 211.25 mL/min µg.

Table 7. Initial levels of elements in natural water sample from Botanga borehole and percentage removal from application of BGM. (Note: Δ increased metal levels after water treatment)

Element	Units	Initial levels	Magnesite %	Bauxite %	Gypsum %	BGM %
Calcium	mg/L	21.1	93.93	40.76	76.3 Δ	67.73
Iron	mg/L	0.00792	93.69	47.22	99.2 Δ	71.09
Magnesium	mg/L	40.8	59.6 Δ	93.38	80.8 Δ	4.66
Potassium	mg/L	27.4	78.87	87.55	71.31	81.39
Silicon	mg/L	22.8	96.75	88.64	13.16	94.39
Sodium	mg/L	202	55.00	84.06	62.43	62.43
Sulfur	mg/L	36.9	45.80	81.68	57.45	3.79
Aluminum	μ g/L	14.6	86.30	77.1 Δ	87.8 Δ	93.4 Δ
Arsenic	μ g/L	92.12	99.92	99.65	98.42	99.86
Barium	μ g/L	27.2	96.32	18.01	71.9 Δ	30.88
Boron	μ g/L	34.7	90.03	25.36	19.31	35.73
Cadmium	μ g/L	0.0978	79.55	79.55	51.6 Δ	79.55
Chromium	μ g/L	154	87.40	5.19	69.48	81.7 Δ
Cobalt	μ g/L	0.54	90.74	81.30	86.4 Δ	82.43
Copper	μ g/L	42.8	99.21	97.45	78.50	99.25
Lead	μ g/L	3.94	99.49	98.25	26.8 Δ	99.49
Manganese	μ g/L	4.49	98.31	85.81	93.1 Δ	92.96
Mercury	μ g/L	2.03	29.5 Δ	34 Δ	29 Δ	36.8 Δ
Molybdenum	μ g/L	4.5	41.33	91.96	32.44	61.11
Nickel	μ g/L	10.4	96.60	94.64	94.3 Δ	92.89
Phosphorus	μ g/L	77.4	97.42	87.30	21.71	95.52
Strontium	μ g/L	405	98.67	78.35	6.5 Δ	88.84
Zinc	μ g/L	630	99.82	99.24	95.44	99.89
Chloride	mg/L	104	63.08	58.08	73.17	56.44
Fluoride	mg/L	2.47	68.58	90.85	76.03	61.82
Nitrates	mg/L	37.7	59.42	83.18	62.07	64.72
Nitrate as N	mg/L	8.52	59.39	83.22	62.21	64.79
Sulfate SO ₄ ²⁻	mg/L	82.2	30.29	75.79	60.71	10.2 Δ

The bauxite column showed good efficiency, as shown in the order of highest removal to the lowest $\geq 59\%$. The element removal ranged from 75.8% sulphate to 99% As and Zn (Table 7). The 71% Al was also released in water. The uptake of As in bauxite (Table 8) was 0.078 μ g/g from the flow rate of 0.57 mL/min. The Thomas kinetic rate constant K_{TH} for As removal at 30 min was 97.39 mL/min μ g (Table 8).

The gypsum uptake was higher at 98.4% for As and 95.4% Zn while other elements removal $\geq 59\%$ ranged between 60.7% sulfate and 78.5% Cu (Table 7). The As adsorption capacity recorded at 30 min was 1.4 μ g/g from the flow-rate of 0.5 mL/min (Table 8). The Thomas kinetic rate constant K_{TH} for As removal at 30 min from the application of gypsum was recorded as 121.45 mL/min μ g (Table 8).

For the BGM, an uptake above 59% was recorded, ranging between 61.1% Mo and 99% of Zn, As, Pb, and Cu (Table 8). Arsenic adsorption capacity at 30 min was 0.1 μ g/g from the flow rate of 0.7 mL/min (Table 8), while the Thomas kinetic rate constant K_{TH} was 29.48 mL/min μ g.

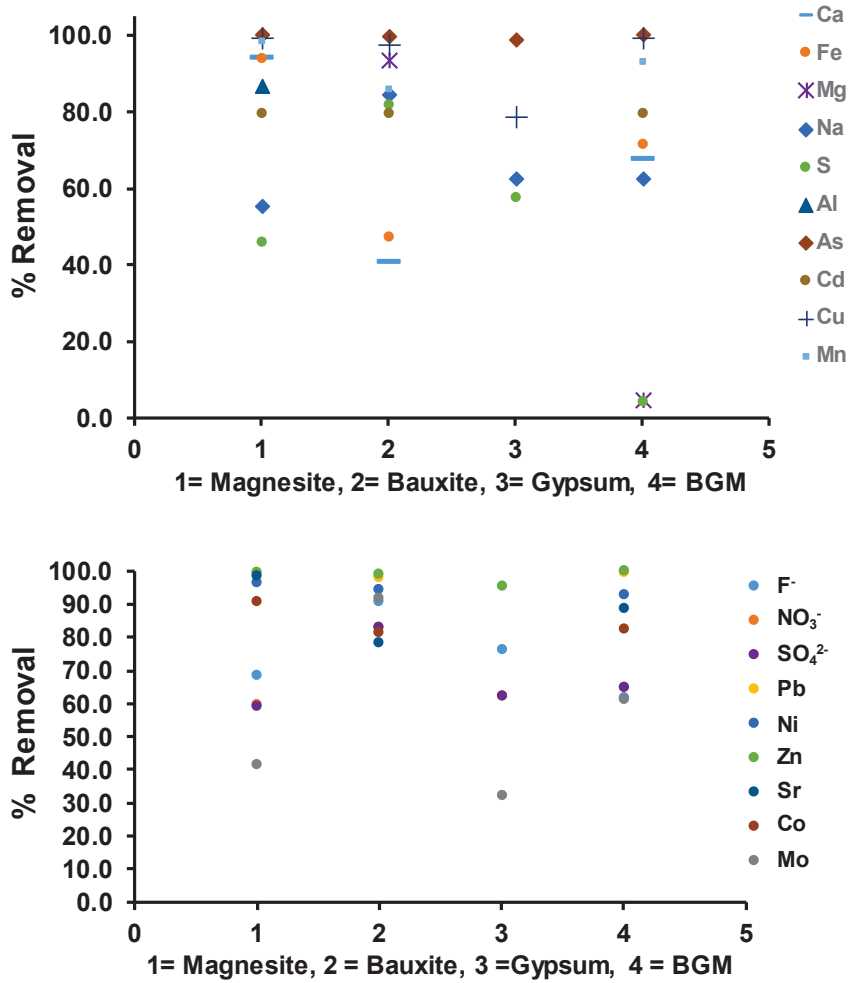


Figure 37. Percentage removal of various elements from natural water sample water from Botanga borehole (Table 7).

Table 8 Arsenic removal in the mini-scale column at 30 min.

parameters	Magnesite	Bauxite	Gypsum	BGM
pH	10	7	9	8
flow rate (mL/min)	1	0.57	0.5	0.7
qt (µg/g)	0.14	0.078	0.07	0.1
K _{TH} (mL/min µg)	211.25	97.39	121.45	29.48
effluent (mL)	30	17	15	20

5.5. NATURAL FACTORS THAT CONTROL ARSENIC IN LAKE VICTORIA BASIN

The uncertainty in the behavior of most samples collected from Geita and Mara around Lake Victoria basin creates curiosity to understand mechanism of As depletion with an increase in storage time. In the field test, most water samples had high As levels, but in the laboratory analysis, 60% of unfiltered samples (acidified and not acidified) from Geita showed less As after storage of three months. The indicator factors were the presence of sulfur and iron in water samples since bacterial activity can be connected to these metals during reduction and oxidation. In the current study, bacteria were not analyzed, but observations are similar to the previously reported behavior by Anand (2022). Despite the samples being acidified, still As was decreasing with storage time, which signifies the presence of bacteria (not included in the analysis) that utilize As as source of energy to survive in acidic water. The acidified filtered samples and unfiltered behaved similarly in As reduction with storage time.

6. DISCUSSION

6.1. OCCURRENCE OF ARSENIC (*PAPER I*)

The review study of As occurrence and spatial distribution in the African environment (*Paper I*) was useful to create awareness and insight into As contamination in African regions where data shows high As levels in surface water compared to groundwater (Irunde *et al.*, 2022).

The data for As contamination in groundwater and surface water published in Africa ranged between maximum and minimum As levels to evaluate percentages that exceed the WHO recommended guideline (Irunde *et al.*, 2023). It was revealed that 86% of maximum As levels in groundwater exceeded the WHO recommended guideline of 0.01 mg/L, and 20% was reported in Tanzania, especially around the gold mining area of Geita and Mara (*Paper I*). It was reported that both natural processes and anthropogenic activities contributed to As distribution in water, soil, sediments, vegetables, and fish in regions of Africa. Climatic change factors such as prolonged drought, flooding, aquifer depth, and land use, such as irrigation, have contributed to As release in the water (Coomar *et al.*, 2019).

In west Africa, more studies revealed the occurrence of health risks from As contamination (Ahoulé *et al.*, 2015). Similarly, health problems have been reported in Tanzania (Nyanza *et al.*, 2019); however, more epidemiological studies are required.

The people of Tanzania were not aware of simple mitigation techniques for As despite the process being well-studied in the world, especially in Bangladesh. Hence, the importance of the present study aims to evaluate locally available materials presented in *Papers III, IV, and V*.

6.2. GEOCHEMICAL EVALUATION OF WATER (*PAPER II*)

The water sample analysis and evaluation using different analytical methods, statistics, and geochemical simulations revealed more contaminated areas from As, which need simple preparation of removal technologies represented in *Papers III, IV, and V*.

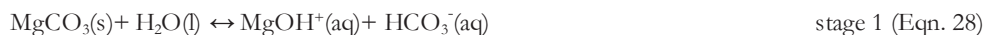
Arsenic concentrations differed within the area due to the geological rock formation in the specific area (*Paper II*). The more contaminated areas, about 80 % were observed within Tarime, while 28% were within Geita (Ligate *et al.*, 2022). The surface water was characterized with more dissolved As(V) than the boreholes, which indicates that the depth affects As release into the water (*Paper II*).

From the depicted Table 2, there was a high dissolved Al in the water, which might be caused by reductive dissolution, and hence high As was released (*Paper II*). The dissolution of metal hydroxides of Al/Fe was evaluated using principal component analysis (PCA) in *Paper II* and revealed positive correlation at *p*-value less than 0.05 (*Paper II*).

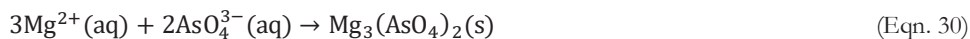
6.3. MAGNESITE (*PAPER III*)

Calcination of magnesite powder sample at the temperature of 500 °C (Xu *et al.*, 2010) is a thermal modification that increases stability on the magnesite surface of active sites for As removal. X-ray diffraction analysis of the magnesite sample showed magnesium carbonate (MgCO₃) as the dominant phase in the material. For the ICP-OES confirmed the raw magnesite to contain iron (Fe), then the other phases in the magnesite were magnesium iron carbonate Mg_{0.99}Fe_{0.01}(CO₃), iron carbonate Fe(CO)₃, and silicon dioxide (SiO₂) (Irunde *et al.*, 2023). The previous reported transformation of metals to oxides under heating were FeCO₃ to Fe₂O₃ at 350°C, 600 °C (Zhao *et al.*, 2014), magnesite to MgO at 1000°C, (Masindi, 2021), 600 °C, 700 °C, and 800°C (Salameh *et al.*, 2015), magnesite to MgO, Fe₂O₃, and CO₂ at 700 °C (Liang *et al.*, 2022). Thus, in the present study, the magnesite converted to products of MgO and Fe₂O₃. Pure MgO was reported to raise water pH to 13 (Natsi *et al.*, 2023), which correlated to the effect of calcined magnesite to raise pH abruptly during As removal in our study.

In the initial pH 1.51, 4, and 7, there was rapid raise in pH up to 10 when calcined magnesite was applied for As removal. The probable causes of the raise in pH were the formation of Mg(OH)₂ (Tong and Tang, 1999) from the dissociation of MgCO₃ (Eqn. 28 and 29) in water (Shadrunkova *et al.*, 2022) and MgO. The formation of oxides of Mg, Fe, and C, after calcination, also raises pH of the water (Liang *et al.*, 2022). The point of zero charge (pHpzc) for Mg(OH)₂ was previously reported to be 12.4 and about 100% As(V) removal at pH 11 without dissolution of Mg(OH)₂ (McNeill and Edwards, 1997). Thus, the alkaline solution in the present study favored As removal at pH 10 since the point of zero charges pHpzc for magnesite was previously reported to be around 11 (Masindi *et al.*, 2014); hence the surface is positively charged to attract negatively As. Furthermore, the metals of Mg, Ca, and Fe in calcined magnesite were not released into the solution at a value higher than WHO except Al, which exceeded the recommended guideline of 0.2 mg/L by 0.1 mg/L.



The mechanism of As uptake by calcined magnesite at pH 10 could be enhanced through precipitation (McNeill and Edwards, 1997) of arsenate (Eqn. 30 and 31). The formation of precipitate phases was also observed when the natural water was simulated in Visual MINTEQ (Irunde *et al.*, 2023). The presence of Fe in calcined magnesite added value to efficient As removal; however, other metals such as titanium, zirconium, zinc, and manganese can improve the synergic effect on As removal (Zhang *et al.*, 2021).



The chemical reaction was predicted as a control factor for As removal when fitted with pseudo-second-order kinetics, which correlates to the previously reported (Bulut and Tez, 2007). The first-order kinetic rate constant in the rate law was observed increasing with an increase in dosage of 0.05 – 5 g/L correlated to the previously first-order kinetic reported (Zhang *et al.*, 2004) and hence indicates slower equilibrium time at low dosage. The rapid intraparticle rate diffusion was exhibited at 0.5 g/L, which deviates from the slow intraparticle rate diffusion reported previously (Chen *et al.*, 2008). The removal isotherm fitted the Freundlich equation, which correlated to the previously reported (Liu *et al.*, 2014) and might highlight the presence of multi-sites as well as mesoporous surface (Xie *et al.*, 2022) that influences As removal.

Arsenic removal percentage increased with an increase in dosage, while removal capacity decreased with an increase in dosage. The removal capacity ranging from 0.006 mg/g to 8.4 mg/g was closer to the adsorption capacity reported (Aredes *et al.*, 2013). The comparison of predicted small error dosage during water treatment using 0.05 g/L and 50 g/L shows that 0.05 g/L is preferential at lower As concentration below 5 mg/L, while 50 g/L was significant at probability <0.001 for treating higher As concentrations. The artificial neural network helped to predict pH as the most important parameter for As removal from water from the application of magnesite.

6.4. BAUXITE (*PAPER IV*)

The 500 °C for the bauxite calcination was previously reported to convert bauxite into oxides (Mohapatra *et al.*, 2008). The present study reports the presence of a large amount of gibbsite phase, while the other phases were aluminium silicate, aluminium oxides, and iron oxides, which enhance As removal from water (*Paper IV*). The presence of iron oxide in the bauxite sample increases fluorescence, which led to the background noise observed in the x-ray diffraction spectra (Fig. 14). The high content of oxygen of 68% signifies high content of aluminium oxides, similar to the previously reported (Mohapatra *et al.*, 2008). The calcination of the bauxite affects porosity and leads to the reduction in surface area, which was not reported by Mohapatra *et al.* (2008).

In natural water, the percentage removal increased with dosage, similar to previously reported (Mohapatra *et al.*, 2008). However, lower pH 4 gave higher As removal, and this declined as the pH increased to 11, which signifies the ligand exchange mechanism of As and fluoride removal (Mohapatra *et al.*, 2008). The increase in hydroxyapatite saturation index with pH improved the removal of fluoride at pH 10. Arsenic species in the water were successfully removed to below WHO recommended guidelines for drinking water.

Arsenic removal increase with an increase in bauxite dosage was previously reported (Mohapatra *et al.*, 2008) and was in agreement with the results from visual MINTEQ. Dosage of 5 g/L was previously reported to enhance As percentage removal up to 99% in 3 hours (Bhakat *et al.*, 2006; Mohapatra *et al.*, 2008). In the present study, the reduction of As to below 0.001 mg/L due to the application of 5 g/L was limited to concentration range of 0.1, 0.5, 1, and 3, while 5.27 mg/L was decreased to below 0.005 mg/L, which is still within WHO recommended guideline for drinking water of 0.01 mg/L. This dosage is sufficient for As removal around gold mining areas in Tanzania, from which it is current As contamination does not exceed 0.3 mg/L. The extended As concentrations between 10 and 30 mg/L were sufficiently treated from application of 50 g/L calcined bauxite. The linear regression revealed that the application of 50 g/L calcined bauxite for As removal exhibited less standard error, making it suitable for longer periods of water treatment. The adsorption capacity decreased with an increase in dosage because more active sites were not saturated.

The increase in initial As concentration decreased the percentage removal of the lower dosage of 0.5 g/L since the active sites were saturated in a short contact time (*Paper IV*). The increase in initial As concentration ranging between 0.1 mg/L and 30 mg/L did not destabilize dosages ranging from 5 g/L and 100 g/L (*Paper IV*). However, the bauxite calcined free from the CO₂ environment exhibited less tolerance to the higher As concentration since the bauxite calcined in the presence of the CO₂ was hypothesized to absorb the CO₂ and exhibited rapid removal up to 99% (*Paper IV*). The adsorption capacity (0.9 - 6.3 mg/g) increases with an increase in initial As (1 - 20 mg/L), similar to the reported (Bhakat *et al.*, 2006), which signifies more active sites are saturated from As (*Paper IV*).

The application of the rate law orders revealed that higher dosages depleted As from the solution in a short equilibrium time, and lower dosages are suitable for lower As concentrations (*Paper IV*). The pseudo-second-order explained the results better, which reveals the involvement of chemical reactions that control As removal from water similar to as previously reported (Bulut and

Tez, 2007). The experimental results fitted Langmuir isotherm with adsorption capacity of 1.33 mg/g, which is closer to the one reported 1.37 and 1.78 mg/g from the application of 5 g/L (Bhakat *et al.*, 2006; Mohapatra *et al.*, 2008).

For the visual, MINTEQ presents that an increase in pH influences decrease in As removal; the acidity nature of bauxite was useful since the higher percentage removal was observed at pH 4 (*Paper IV*). The amphoteric nature of bauxite was confirmed when the pH in acidic solution was slightly raised, and the pH 7 was decreased to 6 (*Paper IV*). In the batch experiment, the linear regression and artificial neural network indicated that pH and contact time were important for As removal. The regeneration of the spent bauxite was leaching much aluminium, which decreased the suitability of the adsorbent use in more than one cycle.

6.5. GYPSUM (*PAPER V*)

Characterization of calcined gypsum revealed the presence of calcium minerals such as CaSO_4 , CaO_3 , and CaO , which raise pH. The pH was previously reported as an important parameter to enhance As removal on a synthesized calcium sulfate (Chen *et al.*, 2014), which correlates to the present study. The percentage removal of As showed efficiency removal at high pH 10 and lower removal at lower pH 4. The increase in pH from 4 to 10 required a small amount of dosage since As removal was increasing with pH. The oversaturation of minerals was also increased with pH, from which precipitated minerals of gypsum, calcite, $\text{Ca}_3(\text{AsO})_2 \cdot 4\text{H}_2\text{O}(\text{s})$, and hydroxyapatite might be contributed to As removal from water. The ionized arsenite dominance was increased with pH up to 95% at pH 10.4. In natural water, As(III) removal was 99%, which deviates from the reported that As(III) was not removed (Chen *et al.*, 2014). The visual MINTEQ simulation revealed the presence of high ionic strength, which lowers the ability for As uptake, similar to the result reported (So *et al.*, 2008).

In the application of calcined gypsum for As removal from a solution prepared in the laboratory, the observation shows percentage removal decreased with an increase in initial As concentrations in the solution (*Paper V*). The synergic contribution of longer contact time and pH 9 enhanced the reduction of As from the water solution (*Paper V*). The behavior of decreasing As removal was previously reported by Chen *et al.* (2014). The decrease in As removal as initial concentration increases has been reported (Rodríguez *et al.*, 2008). The application of 50 g/L calcined gypsum could reduce As closer to the WHO guideline value of 0.01 mg/L for four hours, which indicates gypsum is preferable for removal of the lower As levels (*Paper V*). The removal capacity increased with an increase in initial As concentration, which deviates from the previously hypothesized precipitation, which was supposed to decrease with an increase in initial As concentration (So *et al.*, 2008). The removal capacity being higher as adsorbent dosage decreases was previously observed (Irunde *et al.*, 2023).

The equilibrium time started at 3 hours when 50 g/L calcined gypsum was used to remove 5.3 mg/L from the solution (*Paper V*), which is shorter due to high dosage than the previously reported 12 hours and 25 hours (Chen *et al.*, 2014; So *et al.*, 2008). The adsorption capacity also increases with an increase in contact time, which indicates slow diffusion into the material for higher As concentrations.

The exposure of the active sites enhances the mass transfer driving force for the adsorbate to attach at the surface of the adsorbent (Chen *et al.*, 2014). In the present study, As percentage removal increases with an increase in dosage, which signifies the presence of active sites. For the adsorption capacity, the trend was vice versa, where it decreases with an increase in adsorbent dosage because the adsorbate is depleted by higher dosage.

For the reported pH(pzc) of calcium minerals ranging between 9 and 10 (Sadiq, 1997) can be the reason why the calcined gypsum was still removing As at pH above 9. The visual MINTEQ simulations also revealed high As removal at higher pH 9 (*Paper V*). The most important

parameter in the present study was pH. The study deviated from the previous report that gypsum lowers pH from 9 to 7 (Rodríguez *et al.*, 2008).

Kinetic reactions in the application of gypsum show that the As removal was governed through chemical reactions since it obeys pseudo-second order (*Paper V*). The higher the dosage exhibited, the shorter half-life, the faster rate constant k_2 , and the higher the adsorption capacity. Intraparticle diffusion correlated to the one reported (Bulut and Tez, 2007), and it signifies slow diffusion since the diffusion rate decreases with an increase in dosage despite the difference in initial As concentration. The application of gypsum deviated from the reported data, which fitted Langmuir and extended isotherm models (Chen *et al.*, 2014; Sø *et al.*, 2008).

Gypsum study reported As removal to occur at pH 12 (Chen *et al.*, 2014), which gives the reason for As not leached at pH 12.47 when 0.1M NaOH was applied to regenerate spent material. The calcium was not leached into the water, which signifies gypsum stabilizes As and is hence suitable for As control in the environment.

The most important parameter for As removal using calcined gypsum was pH, which was significant at p -value of <0.001 . The dosage of 100 g/L indicated less standard error during simulation, and hence, it is the best system for As removal at lower As concentrations below 1 mg/L.

6.6. MINI-SCALE COLUMN EVALUATION

The local material evaluation on mini-scale column (Fig. 36) shows important information, which requires more investigations in future column studies. The ration of (1:1:2) of the local materials in the column, where bauxite is higher in amount slightly regulated pH, which was neutral at the bauxite column, and higher in magnesite and gypsum. The regulation of pH from the application of bauxite is in agreement with the project hypothesis. The flow rate was lower than the previously reported from more porous materials (Roy *et al.*, 2013), and magnesite revealed higher flow rate of 1 mL/min than other columns. The adsorption capacity is in agreement with batch experiments of a similar study. The Thomas kinetic linear equation revealed that the rate flow in the column was higher when the magnesite was applied.

6.7. NATURAL MITIGATION OF ARSENIC

The field study observation leads to the assumption that the arsenic sources around gold mining areas of Geita and Mara are released from the natural sources (oxidation of arsenopyrites) and human activities, such as mining, farming, cattle keeping, and timber conservation. However, many of the natural environments seem to be resourceful for the natural mitigation of As, and this is why there were places where there were very low recorded As concentrations. A high number of water samples from Geita and less number from Mara showed very low As levels so these can be recommended as an alternative source of aquifers that are free from Arsenic contamination for water supply in the mining areas.

During the water sample collection, it was observed that water contained high iron and sulfide. There were abandoned boreholes due to bad odour, and other abandoned boreholes due to the change of color, after the water was pumped out from the borehole into the basket. This was evident that the environment contains high iron, and sulfide, which can be of importance to capture arsenic depending on pH and redox of the specific aquifer.

Alongside the presence of iron, and sulphate, water sources also have a presence of bacteria, which can play part in arsenic oxidation or reduction. In the reducing environment, iron will be reduced to iron (II), which releases As into the water; however, sulfide will be reduced to an insoluble material, which can form complexes with As, and reduces As levels from the environment. For oxidizing environment, sulfide will be oxidized to release As, while Fe is oxidized to an insoluble material that can precipitate As from water.

The presence of bacteria will help in the detoxification of As through the formation of organo-arsenicals, such as dimethylarsenite, which are believed less harmful.

7. CONCLUSIONS

The present study aimed to create awareness and scientific insights about As contamination in the environment, using limited studies conducted in the African continent (*Paper I*). The study includes geochemical evaluation of water sample characteristics in Geita and Mara, where 80% of the As contamination was reported in Mara (*Paper II*). Levels of As about 300 µg/L were reported at locations in Geita and Mara, including several wells in Geita, which were abandoned due to strong odour from sulfide and red color from iron. The Mara region was more contaminated by As, with As(V) being a dominant species, signifying an oxidizing environment. The low contamination in Geita correlates to the natural control of As mobilization, whereby iron and sulfide contribute to bind arsenic when the oxidation and reduction conditions are favourable. The saturation indexes from simulation of natural samples using Visual MINTEQ revealed pH as a main controlling factor in the oxidizing environment, which influences oversaturation of minerals that contain arsenic. The environmental disturbance through natural weathering and human-induced activities leads to the As release in water sources. Increased number of cancer cases from patients originating from the Lake Victoria basin, including regions of Geita and Mara, is a serious indicator, which requires clinical investigations.

Arsenic removal evaluation was described in *Papers III, IV, and V*. The application of calcined magnesite gave a high uptake of As, resulting in levels below the 0.01 mg/L recommended in WHO guidelines for drinking water. The calcined bauxite removed As above 5.3 mg/L to below the 0.01 mg/L at higher dosage of 50 g/L, while lower dosage of 0.5 g/L was suitable for removal of As concentrations below 1 mg/L (*Paper IV*). The application of gypsum is recommended for lower As levels below 0.5 mg/L (*Paper V*). The elements released into the water during treatment and leaching of spent materials were below WHO guidelines, which signify the safety of the materials. The leaching process with an alkaline solution did not leach As from magnesite and gypsum due to formation of strong bond between Mg-O-As and Ca-O-As. The alkaline solution leached much Al from bauxite, reducing its uptake capacity after one period of treatment. Elucidation of the mechanisms of As uptake in magnesite, gypsum, and bauxite requires more advanced techniques to reveal bonding of As to the surfaces of the material.

Experiments with a mini-scale column showed that a fast flow rate can be viable for the use of magnesite for As removal, and there is a potential to upscale this technique. The mini-scale column showed that bauxite has the potential to regulate the pH of the solution in the treatment system. More studies on the materials represented in this study are recommended to determine their useful lifetime before the necessary replacement in the column.

8. REFERENCES

- Abiye, T.A., Bhattacharya, P., 2019. Arsenic concentration in groundwater: Archetypal study from South Africa. *Groundw. Sustain. Dev.* 9, 100246. <https://doi.org/10.1016/j.jgsd.2019.100246>
- Ahmad, A., Richards, L.A., Bhattacharya, P., 2017. Arsenic remediation of drinking water: an overview. In: P. Bhattacharya, D.A. Polya & D. Jovanovic (Eds.) *Best Practice Guide on the Control of Arsenic in Drinking Water*. Metals and Related Substances in Drinking Water Series. IWA Publishing, UK, pp. 79–98. https://doi.org/10.2166/9781780404929_079
- Ahmad, A., van der Wal, A., Bhattacharya, P., van Genuchten, C.M., 2019. Characteristics of Fe and Mn bearing precipitates generated by Fe(II) and Mn(II) co-oxidation with O₂, MnO₄ and HOCl in the presence of groundwater ions. *Water Res.* 161, 505–516. <https://doi.org/10.1016/j.watres.2019.06.036>

- Ahoulé, D.G., Lalanne, F., Mendret, J., Brosillon, S., Maïga, A.H., 2015. Arsenic in African waters: A review. *Water. Air. Soil Pollut.* 226. <https://doi.org/10.1007/s11270-015-2558-4>
- Aredes, S., Klein, B., Pawlik, M., 2013. The removal of arsenic from water using natural iron oxide minerals. *J. Clean. Prod.* 60, 71–76. <https://doi.org/10.1016/j.jclepro.2012.10.035>
- Asante, K.A., Agusa, T., Biney, C.A., Agyekum, W.A., Bello, M., Otsuka, M., Itai, T., Takahashi, S., Tanabe, S., 2012. Multi-trace element levels and arsenic speciation in urine of e-waste recycling workers from Agbogbloshie, Accra in Ghana. *Sci. Total Environ.* 424, 63–73. <https://doi.org/10.1016/j.scitotenv.2012.02.072>
- Bakatula, E.N., Molaudzi, R., Nekhunguni, P., Tutu, H., 2017. The removal of arsenic and uranium from aqueous solutions by sorption onto Iron Oxide-Coated Zeolite (IOCZ). *Water. Air. Soil Pollut.* 228. <https://doi.org/10.1007/s11270-016-3190-7>
- Bardelli, F., Benvenuti, M., Costagliola, P., Di Benedetto, F., Lattanzi, P., Meneghini, C., Romanelli, M., Valenzano, L., 2011. Arsenic uptake by natural calcite: An XAS study. *Geochim. Cosmochim. Acta* 75, 3011–3023. <https://doi.org/10.1016/j.gca.2011.03.003>
- Bhakat, P.B., Gupta, A.K., Ayoob, S., Kundu, S., 2006. Investigations on arsenic(V) removal by modified calcined bauxite. *Colloids Surfaces A Physicochem. Eng. Asp.* 281, 237–245. <https://doi.org/10.1016/j.colsurfa.2006.02.045>
- Bhattacharya, P., Jacks, G., Ahmed, K.M., Routh, J., Khan, A.A., 2002. Arsenic in groundwater of the Bengal Delta Plain aquifers in Bangladesh. *Bull. Environ. Contam. Toxicol.* 69, 538–545. <https://doi.org/10.1007/s00128-002-0095-5>
- Bhattacharya, P., Samal, A.C., Majumdar, J., Santra, S.C., 2010. Arsenic contamination in rice, wheat, pulses, and vegetables: A study in an arsenic affected area of West Bengal, India. *Water. Air. Soil Pollut.* 213, 3–13. <https://doi.org/10.1007/s11270-010-0361-9>
- Bretzler, A., Stolze, L., Nikiema, J., Lalanne, F., Ghadiri, E., Brennwald, M.S., Rolle, M., Schirmer, M., 2019. Hydrogeochemical and multi-tracer investigations of arsenic-affected aquifers in semi-arid West Africa. *Geosci. Front.* 10, 1685–1699. <https://doi.org/10.1016/j.gsf.2018.06.004>
- Bulut, Y., Tez, Z., 2007. Adsorption studies on ground shells of hazelnut and almond. *J. Hazard. Mater.* 149, 35–41. <https://doi.org/10.1016/j.jhazmat.2007.03.044>
- Bundschuh, J., Maity, J.P., Nath, B., Baba, A., Gunduz, O., Kulp, T.R., Jean, J.S., Kar, S., Yang, H.J., Tseng, Y.J., Bhattacharya, P., Chen, C.Y., 2013. Naturally occurring arsenic in terrestrial geothermal systems of western Anatolia, Turkey: Potential role in contamination of freshwater resources. *J. Hazard. Mater.* 262, 951–959. <https://doi.org/10.1016/j.jhazmat.2013.01.039>
- Chen, H., Liu, L., Gong, R., Wei, R., Yi, Q., Qiu, A., 2016. Comparison of Kinetics of Arsenic(V) Adsorption on Two Types of Red Soil Weathered from Granite and Sandstone. *Water. Air. Soil Pollut.* 227. <https://doi.org/10.1007/s11270-016-3107-5>
- Chen, X., Yang, L., Zhang, J., Huang, Y., 2014. Exploration of As(III)/As(V) uptake from aqueous solution by synthesized calcium sulfate Whisker. *Chinese J. Chem. Eng.* 22, 1340–1346. <https://doi.org/10.1016/j.cjche.2014.09.018>
- Chen, Y.-N., Chai, L.-Y., Shu, Y.-D., 2008. Study of arsenic(V) adsorption on bone char from aqueous solution. *J. Hazard. Mater.* 160, 168–172. <https://doi.org/10.1016/j.jhazmat.2008.02.120>
- Chiban, M., Soudani, A., Sinan, F., Persin, M., 2011. Single, binary and multi-component adsorption of some anions and heavy metals on environmentally friendly *Carpobrotus edulis*

- plant. *Colloids Surfaces B Biointerfaces* 82, 267–276. <https://doi.org/10.1016/j.colsurfb.2010.09.013>
- Chung, J.Y., Yu, S. Do, Hong, Y.S., 2014. Environmental source of arsenic exposure. *J. Prev. Med. Public Heal.* 47, 253–257. <https://doi.org/10.3961/jpmph.14.036>
- Coomar, P., Mukherjee, A., Bhattacharya, P., Bundschuh, J., Verma, S., Fryar, A.E., Ramos Ramos, O.E., Muñoz, M.O., Gupta, S., Mahanta, C., Quino, I., Thunvik, R., 2019. Contrasting controls on hydrogeochemistry of arsenic-enriched groundwater in the homologous tectonic settings of Andean and Himalayan basin aquifers, Latin America and South Asia. *Sci. Total Environ.* 689, 1370–1387. <https://doi.org/10.1016/j.scitotenv.2019.05.444>
- Cotruvo, J.A., 2017. WHO guidelines for drinking water quality: first addendum to the fourth edition. *J. Am. Water Works Assoc.* 109, 44–51. <https://doi.org/10.5942/jawwa.2017.109.0087>
- Cumbal, L., Sengupta, A.K., 2005. Arsenic removal using polymer-supported hydrated iron(III) oxide nanoparticles: Role of Donnan membrane effect. *Environ. Sci. Technol.* 39, 6508–6515. <https://doi.org/10.1021/es050175e>
- El-Badry, A.E.M.A., Khalifa, M.M., 2017. The occurrence and distribution of high-arsenic, selenium, tin and antimony in bottom sediments of Burullus lagoon and its effects on human health, Egypt. *J. African Earth Sci.* 136, 305–311. <https://doi.org/10.1016/j.jafrearsci.2017.08.001>
- Gbogbo, F., Otoo, S.D., Asomaning, O., Huago, R.Q., 2017. Contamination status of arsenic in fish and shellfish from three river basins in Ghana. *Environ. Monit. Assess.* 189. <https://doi.org/10.1007/s10661-017-6118-9>
- Gustafsson, J.P., 2022. *Visual MINTEQ Program Version 3.1.* <http://vminteq.com>
- Han, Y.S., Ji, S., Lee, P.K., Oh, C., 2017. Bauxite residue neutralization with simultaneous mineral carbonation using atmospheric CO₂. *J. Hazard. Mater.* 326, 87–93. <https://doi.org/10.1016/j.jhazmat.2016.12.020>
- Herath, I., Vithanage, M., Bundschuh, J., Maity, J.P., Bhattacharya, P., 2016. Natural arsenic in global groundwaters: distribution and geochemical triggers for mobilization. *Curr. Pollut. Reports* 2, 68–89. <https://doi.org/10.1007/s40726-016-0028-2>
- Irunde, R., Ijumulana, J., Ligate, F., Maity, J.P., Ahmad, A., Mtamba, J., Mtalo, F., Bhattacharya, P., 2022. Arsenic in Africa: Potential sources, spatial variability, and the state of the art for arsenic removal using locally available materials. *Groundw. Sustain. Dev.* 18, 100746. <https://doi.org/10.1016/j.gsd.2022.100746>
- Irunde, R., Ligate, F.J., Ijumulana, J., Ahmad, A., Maity, J.P., Hamisi, R., Philip, J.Y.N., Kilulya, K.F., Karlton, E., Mtamba, J., Bhattacharya, P., Mtalo, F., 2023. The natural magnesite efficacy on arsenic extraction from water and alkaline influence on metal release in water. *Appl. Geochem.* 155, 105705. <https://doi.org/10.1016/j.apgeochem.2023.105705>
- Kapaj, S., Peterson, H., Liber K., Bhattacharya, P., 2006. Human health effects from chronic arsenic poisoning – A Review. *J. Environ. Sci. Health, Part A.* 41(10), 2399–2428. <https://doi.org/10.1080/10934520600873571>
- Kassenga, G., Mato, R., 2008. Arsenic contamination levels in drinking water sources in mining areas in Lake Victoria Basin, Tanzania, and its removal using stabilized ferralsols. *Int. J. Biol. Chem. Sci.* 2, 389–400. <https://doi.org/10.4314/ijbcs.v2i4.39771>
- Kinyondo, A., Huggins, C., 2021. Promoting environmental sustainability in the artisanal and small-scale mining sector in Tanzania. 2021/119. <https://doi.org/10.35188/UNU-WIDER/2021/059-7>

- Leuenberger, A., Kihwele, F., Lyatuu, I., Kengia, J.T., Farnham, A., Winkler, M.S., Merten, S., 2021. Gendered health impacts of industrial gold mining in northwestern Tanzania: perceptions of local communities. *Impact Assess. Proj. Apprais.* 39, 183–195. <https://doi.org/10.1080/14615517.2021.1904697>
- Liang, H., Guo, P., Yang, Y., Wang, W., Sun, Z., 2022. Environmental application of engineering magnesite slag for phosphate adsorption from wastewater. *Environ. Sci. Pollut. Res.* 29, 59502–59512. <https://doi.org/10.1007/s11356-022-20029-z>
- Ligate, F., Lucca, E., Ijumulana, J., Irunde, R., Kimambo, V., Mtamba, J., Ahmad, A., Hamisi, R., Prakash, J., Mtaló, F., 2022. Geogenic contaminants and groundwater quality around Lake Victoria goldfields in northwestern Tanzania. *Chemosphere* 307, 135732. <https://doi.org/10.1016/j.chemosphere.2022.135732>
- Liu, Jing, Huang, X., Liu, Juan, Wang, W., Zhang, W., Dong, F., 2014. Adsorption of arsenic(V) on bone char: Batch, column and modeling studies. *Environ. Earth Sci.* 72, 2081–2090. <https://doi.org/10.1007/s12665-014-3116-x>
- Macháček, J., 2019. Typology of environmental impacts of artisanal and small-scale mining in African Great Lakes Region. *Sustainability.* 11, 1–24. <https://doi.org/10.3390/su11113027>
- Maity, J.P., Chen, C.Y., Bhattacharya, P., Sharma, R.K., Ahmad, A., Patnaik, S., Bundschuh, J., 2021. Advanced application of nano-technological and biological processes as well as mitigation options for arsenic removal. *J. Hazard. Mater.* 405, 123885. <https://doi.org/10.1016/j.jhazmat.2020.123885>
- Maity, J.P., Nath, B., Chen, C.Y., Bhattacharya, P., Sracek, O., Bundschuh, J., Kar, S., Thunvik, R., Chatterjee, D., Ahmed, K.M., Jacks, G., Mukherjee, A.B., Jean, J.S., 2011. Arsenic-enriched groundwaters of India, Bangladesh and Taiwan: Comparison of hydrochemical characteristics and mobility constraints. *J. Environ. Sci. Heal. - Part A Toxic/Hazardous Subst. Environ. Eng.* 46, 1163–1176. <https://doi.org/10.1080/10934529.2012.598711>
- Masindi, V., 2021. Conversion of cryptocrystalline magnesite to MgO nanosheets: Insights into microstructural properties. *Mater. Today Proc.* 38, 1077–1087. <https://doi.org/10.1016/j.matpr.2020.06.072>
- Masindi, V., Gitari, M.W., Tutu, H., De Beer, M., 2014. Application of magnesite–bentonite clay composite as an alternative technology for removal of arsenic from industrial effluents. *Toxicol. Environ. Chem.* 96, 1435–1451. <https://doi.org/10.1080/02772248.2014.966714>
- Masindi, V., Gitari, W.M., 2016. Removal of arsenic from wastewaters by cryptocrystalline magnesite: Complimenting experimental results with modelling. *J. Clean. Prod.* 113, 318–324. <https://doi.org/10.1016/j.jclepro.2015.11.043>
- Mata-Perez, F., Perez-Benito, J.F., 1987. The kinetic rate law for autocatalytic reactions. *J. Chem. Educ.* 64, 925–927. <https://doi.org/10.1021/ed064p925>
- McNeill, L.S., Edwards, M., 1997. Arsenic removal during precipitative softening. *J. Environ. Eng.* 123, 453–460. [https://doi.org/10.1061/\(asce\)0733-9372\(1997\)123:5\(453\)](https://doi.org/10.1061/(asce)0733-9372(1997)123:5(453))
- Mohapatra, D., Mishra, D., Park, K.H., 2008. A laboratory scale study on arsenic(V) removal from aqueous medium using calcined bauxite ore. *J. Environ. Sci.* 20, 683–689. [https://doi.org/10.1016/S1001-0742\(08\)62113-0](https://doi.org/10.1016/S1001-0742(08)62113-0)
- Natsi, P.D., Goudas, K.-A., Koutsoukos, P.G., 2023. Phosphorus recovery from municipal wastewater: brucite from MgO hydrothermal treatment as magnesium source. *Crystals* 13, 208. <https://doi.org/10.3390/cryst13020208>
- Nriagu, J., Bhattacharya, P., Mukherjee, A., Bundschuh, J., Zevenhoven, R., Loeppert, R., 2007.

- Arsenic in soil and groundwater: an overview. In: P. Bhattacharya, A.B. Mukherjee, J. Bundschuh, R. Zevenhoven, R.H. Loeppert. (Eds.) *Arsenic in Soil and Groundwater Environment: Biogeochemical Interactions, Health Effects and Remediation*, Trace Metals and other Contaminants in the Environment, Volume 9, Elsevier B.V. Amsterdam, The Netherlands, pp. 3–60. [https://doi.org/10.1016/s0927-5215\(06\)09001-1](https://doi.org/10.1016/s0927-5215(06)09001-1)
- Nyanza, E.C., Bernier, F.P., Manyama, M., Hatfield, J., Martin, J.W., Dewey, D., 2019. Maternal exposure to arsenic and mercury in small-scale gold mining areas of Northern Tanzania. *Environ. Res.* 173, 432–442. <https://doi.org/10.1016/j.envres.2019.03.031>
- Nyanza, E.C., Dewey, D., Thomas, D.S.K., Davey, M., Ngallaba, S.E., 2014. Spatial distribution of mercury and arsenic levels in water, soil and cassava plants in a community with long history of gold mining in Tanzania. *Bull. Environ. Contam. Toxicol.* 93, 716–721. <https://doi.org/10.1007/s00128-014-1315-5>
- Ogola, J.S., Mitullah, W. V, Omulo, M.A., 2002. Impact of gold mining on the environment and human health: A case study in the Migori gold belt, Kenya. *Environ. Geochem. Health* 24, 141–157. <https://doi.org/10.1023/A:1014207832471>
- Rango, T., Bianchini, G., Beccaluva, L., Tassinari, R., 2010. Geochemistry and water quality assessment of central Main Ethiopian Rift natural waters with emphasis on source and occurrence of fluoride and arsenic. *J. African Earth Sci.* 57, 479–491. <https://doi.org/10.1016/j.jafrearsci.2009.12.005>
- Rango, T., Vengosh, A., Dwyer, G., Bianchini, G., 2013. Mobilization of arsenic and other naturally occurring contaminants in groundwater of the main ethiopian rift aquifers. *Water Res.* 47, 5801–5818. <https://doi.org/10.1016/j.watres.2013.07.002>
- Rodríguez, J.D., Jiménez, A., Prieto, M., Torre, L., García-Granda, S., 2008. Interaction of gypsum with As(V)-bearing aqueous solutions: surface precipitation of guerinite, sainfeldite, and $\text{Ca}_2\text{NaH}(\text{AsO}_4)_2 \cdot 6\text{H}_2\text{O}$, a synthetic arsenate. *Am. Mineral.* 93, 928–939. <https://doi.org/10.2138/am.2008.2750>
- Román-Ross, G., Cuello, G.J., Turrillas, X., Fernández-Martínez, A., Charlet, L., 2006. Arsenite sorption and co-precipitation with calcite. *Chem. Geol.* 233, 328–336. <https://doi.org/10.1016/j.chemgeo.2006.04.007>
- Roy, P., Mondal, N.K., Bhattacharya, S., Das, B., Das, K., 2013. Removal of arsenic(III) and arsenic(V) on chemically modified low-cost adsorbent: batch and column operations. *Appl. Water Sci.* 3, 293–309. <https://doi.org/10.1007/s13201-013-0082-5>
- Rusibamayila, M., Meshi, E., Mamuya, S., 2018. Respiratory impairment and personal respirable dust exposure among the underground and open cast gold Miners in Tanzania. *Ann. Glob. Heal.* 84, 419–428. <https://doi.org/10.29024/aogh.2323>
- Rwiza, M.J., Focus, E., Bayuo, J., Kimaro, J.M., Kleinke, M., Lyasenga, T.J., Mosses, J.T., Marwa, J., 2023. Artisanal and small-scale mining in Tanzania and health implications: A policy perspective. *Helijon* 9, e14616. <https://doi.org/10.1016/j.helijon.2023.e14616>
- Sadik, C., Moudden, O., El Bouari, A., El Amrani, I.E., 2016. Review on the elaboration and characterization of ceramics refractories based on magnesite and dolomite. *J. Asian Ceram. Soc.* 4, 219–233. <https://doi.org/10.1016/j.jascr.2016.06.006>
- Sadiq, M., 1997. Arsenic chemistry in soils : An overview of thermodynamic predictions and field observations. *Water; Air, Soil Pollut.* 93, 117–136.
- Salameh, Y., Albadarin, A.B., Allen, S., Walker, G., Ahmad, M.N.M., 2015. Arsenic(III,V) adsorption onto charred dolomite: Charring optimization and batch studies. *Chem. Eng. J.* 259, 663–671. <https://doi.org/10.1016/j.cej.2014.08.038>

- Salje, E., 1988. Kinetic rate laws as derived from order parameter theory I: Theoretical concepts. *Phys. Chem. Miner.* 15, 336–348. <https://doi.org/10.1007/BF00311038>
- Shadrúnova, I. V., Orekhova, N.N., Stefunko, M.S., 2022. Intensification of the wastewater treatment process using magnesium-containing materials. *IOP Conf. Ser. Earth Environ. Sci.* 1061, 0–8. <https://doi.org/10.1088/1755-1315/1061/1/012029>
- Sø, H.U., Postma, D., Jakobsen, R., Larsen, F., 2008. Sorption and desorption of arsenate and arsenite on calcite. *Geochim. Cosmochim. Acta* 72, 5871–5884. <https://doi.org/10.1016/j.gca.2008.09.023>
- Sun, X., Mao, M., Lu, K., Hu, Q., Liu, W., Lin, Z., 2022. One-step removal of high-concentration arsenic from wastewater to form Johnbaumite using arsenic-bearing gypsum. *J. Hazard. Mater.* 424, 127585. <https://doi.org/10.1016/j.jhazmat.2021.127585>
- Tahmasebpour, M., Hosseini Nami, S., Khatamian, M., Sanaei, L., 2022. Arsenate removal from contaminated water using Fe₂O₃-clinoptilolite powder and granule. *Environ. Technol. (United Kingdom)* 43, 116–130. <https://doi.org/10.1080/09593330.2020.1779821>
- WHO, 2017. *Guidelines for Drinking-Water Quality. 4th Edition.* World Health Organization, Geneva. 631p.
- Tong, L., Tang, M., 1999. Expansion mechanism of alkali-dolomite and alkali-magnesite reaction. *Cem. Concr. Compos.* 21, 361–373. [https://doi.org/10.1016/S0958-9465\(99\)00022-0](https://doi.org/10.1016/S0958-9465(99)00022-0)
- Xie, X., Lu, C., Xu, R., Yang, X., Yan, L., Su, C., 2022. Arsenic removal by manganese-doped mesoporous iron oxides from groundwater: Performance and mechanism. *Sci. Total Environ.* 806, 150615. <https://doi.org/10.1016/j.scitotenv.2021.150615>
- Xu, Y., Dai, Y., Zhou, J., Xu, Z.P., Qian, G., Lu, G.Q.M., 2010. Removal efficiency of arsenate and phosphate from aqueous solution using layered double hydroxide materials: Intercalation vs. precipitation. *J. Mater. Chem.* 20, 4684–4691. <https://doi.org/10.1039/b926239c>
- Yadav, V.S., Prasad, M., Khan, J., Amritphale, S.S., Singh, M., Raju, C.B., 2010. Sequestration of carbon dioxide (CO₂) using red mud. *J. Hazard. Mater.* 176, 1044–1050. <https://doi.org/10.1016/j.jhazmat.2009.11.146>
- Yang, Y., Wei, L., Cui, L., Zhang, M., Wang, J., 2017. Profiles and Risk Assessment of Heavy Metals in Great Rift Lakes, Kenya. *Clean - Soil, Air, Water* 45. <https://doi.org/10.1002/clen.201600825>
- Zhang, T., Zhao, Y., Kang, S., Bai, H., Song, G., Zhang, Q., 2021. Enhanced arsenic removal from water by mechanochemical synthesis of Ca–Al–Fe ternary composites. *J. Clean. Prod.* 321, 128959. <https://doi.org/10.1016/j.jclepro.2021.128959>
- Zhang, W., Singh, P., Paling, E., Delides, S., 2004. Arsenic removal from contaminated water by natural iron ores. *Miner. Eng.* 17, 517–524. <https://doi.org/10.1016/j.mineng.2003.11.020>
- Zhao, K., Guo, H., Zhou, X., 2014. Adsorption and heterogeneous oxidation of arsenite on modified granular natural siderite: characterization and behaviors. *Appl. Geochem.* 48, 184–192. <https://doi.org/10.1016/j.apgeochem.2014.07.016>